

Fig. 4. Akt/GSK-3 $\beta$  signaling regulates the proliferation and survival of hCSCs. (A,B) Phosphorylation of Akt (A) and GSK-3 $\beta$  (B) induced by EGF/bFGF in hCSCs. After serum starvation for 2 h, hCSCs were treated with EGF/bFGF for the period of time indicated. (C) Activation of Akt induced by EGF/bFGF treatment for 5 min was abolished by the pretreatment of Akt-I for 4 h in a dose-dependent manner. (D) Phosphorylation of GSK-3 $\beta$  (inactive) induced by EGF/bFGF treatment for 5 min was enhanced by the pretreatment of 10 nM BIO for 4 h. (E,F) Size distribution of cardiospheres cultured in EGF/bFGF-containing medium in the presence of either 10  $\mu$ M Akt-I (E), or 10 nM BIO (F) for 6 days ( $n = 7$ ). \* $p < 0.01$  and † $p < 0.05$  versus DMSO control. (G,H) TUNEL assay (G) and Ki67 staining (H) of cardiospheres exposed to 10  $\mu$ M Akt-I and 10 nM BIO. Ki67, red. DAPI, blue. \* $p < 0.01$  versus DMSO control ( $n = 3$ ). Scale bars, 50  $\mu$ m.

increase in the number of Ki67-positive cells was observed in cardiospheres exposed to BIO (Fig. 4H).

## Discussion

Our present study provides the novel evidence that hCSCs exhibit a mesenchymal cell-like property and Akt/GSK-3 $\beta$  signaling is involved in their proliferation and sur-

vival. Furthermore, our study shows that hCSCs are predominantly present in the right atrium and outflow tract of the heart (more expressed in infant heart rather than adult heart).

A recent report has suggested that cellular aging induces a functional impairment of mCSC growth that may result from the reduction in Akt phosphorylation and telomerase inactivation [18]. Consistent with these data, we showed

here less telomerase activity in hCSCs from the adult heart than that from the infant heart. The abundance of hCSCs isolated from RA and OFT may reflect their specific distribution in the human heart. Although there is a possibility of bias caused by the patients' background, including disease, age, and sex, our results are consistent with a recent report showing that the stem cell niches are predominantly present in the atrium in the murine heart [19].

Messina et al. [7] have demonstrated that hCSCs can be isolated from human heart using floating culture system. We employed the essentially similar method to isolate hCSCs. However, in contrast to the previous report, we found that c-kit expression was extremely low in the isolated cells from both infant and adult hearts. Several reports demonstrated that c-kit expression was diminished on the lineage-committed cardiac progeny as observed in murine cardiac progenitor cells and cardioblasts [3,5,19]. It is possible that cardiospheres contain a mixed population of cells that, as in the niche, can promote the viability of c-kit progenitors and contribute to their proliferation [7]. Our observation suggest that mixed progenitor populations may exist during the process of lineage-commitment of hCSCs in the human heart as during hematopoietic homeostasis [20].

It is notable that hCSCs have a mesenchymal-like character. Mesenchymal stem cells were conventionally isolated from bone marrow and the presence in many tissues but not heart has recently been reported [21]. In the developing heart, the neural crest cells are known to migrate into the cardiac outflow tract to supply the cells from the primitive epicardial epithelium through a process of epithelial-to-mesenchymal transition [22]. These epicardially derived cells have a mesenchymal phenotype and stem cell property in human adult hearts [23]. Thus, it may be conceivable that hCSCs isolated from the human heart might be originated from the primitive epicardial epithelium.

The mechanism to regulate the proliferation and survival of stem cells has been examined. Akt is a nodal signaling kinase linked to both the proliferation and survival of somatic stem or progenitor cells in neural tissue and blood [24,25]. Our studies demonstrate that the proliferation of hCSCs appears to be dependent on the activation of Akt in response to EGF/bFGF stimulation. Furthermore, we have documented that inhibition of Akt pathway impairs cell growth and survival. Our observations are consistent with two independent studies demonstrating that *ex vivo* transduction of Akt prevents bone marrow-derived MSCs from the oxidative stress-induced apoptosis [10] and that the nuclear-targeting of Akt leads to an acceleration of mCSC expansion [13].

The novel finding we showed here that GSK-3 $\beta$  is also associated with the proliferation and survival of hCSCs may provide the new prospect for stem cell therapy. GSK-3 $\beta$  is one of the substrates of Akt and participates in regulating the cell cycle in various cell types [26]. We found that BIO stimulated the growth kinetics of hCSCs consistent with the observation seen in BIO-mediated pro-

liferation of differentiated cardiomyocytes [27]. Thus, our findings suggest that Akt/GSK-3 $\beta$  pathway is crucial in hCSC growth and survival as well as mCSCs.

In conclusion, the present study demonstrates that the resident CSCs in human hearts have mesenchymal characteristics and proliferate through Akt/GSK-3 $\beta$  pathway. Understanding whether pharmacological inhibition of GSK3 $\beta$  by BIO may act through direct activation of the Wnt signaling pathway for stem cell maintenance [28] will provide a new insight into the signaling pathways required for hCSC expansion and engraftment *in vivo*. These novel findings may enable practical applications for establishing hCSC lines and provide an advanced cell therapy for patients with heart failure.

### Acknowledgments

We thank Y. Yoshida, A. Kosugi, and M. Nishikawa for technical assistance. This work was supported by Grants-in-Aid from the Ministry of Education, Culture, Sports, Science and Technology of Japan, and by Grants-in-Aid from the Ministry of Health, Labor, and Welfare of Japan.

### References

- [1] F. Quaini, K. Urbanek, A.P. Beltrami, N. Finato, C.A. Beltrami, B. Nadal-Ginard, J. Kajstura, A. Leri, P. Anversa, Chimerism of the transplanted heart, *N. Engl. J. Med.* 346 (2002) 5–15.
- [2] P. Anversa, B. Nadal-Ginard, Myocyte renewal and ventricular remodelling, *Nature* 415 (2002) 240–243.
- [3] H. Oh, S.B. Bradfute, T.D. Gallardo, T. Nakamura, V. Gaussin, Y. Mishina, J. Pocius, L.H. Michael, R.R. Behringer, D.J. Garry, M.L. Entman, M.D. Schneider, Cardiac progenitor cells from adult myocardium: homing, differentiation, and fusion after infarction, *Proc. Natl. Acad. Sci. USA* 100 (2003) 12313–12318.
- [4] A.P. Beltrami, L. Barlucchi, D. Torella, M. Baker, F. Limana, S. Chimenti, H. Kasahara, M. Rota, E. Musso, K. Urbanek, A. Leri, J. Kajstura, B. Nadal-Ginard, P. Anversa, Adult cardiac stem cells are multipotent and support myocardial regeneration, *Cell* 114 (2003) 763–776.
- [5] K.L. Laugwitz, A. Moretti, J. Lam, P. Gruber, Y. Chen, S. Woodard, L.Z. Lin, C.L. Cai, M.M. Lu, M. Reth, O. Platoshyn, J.X. Yuan, S. Evans, K.R. Chien, Postnatal isl1+ cardioblasts enter fully differentiated cardiomyocyte lineages, *Nature* 433 (2005) 647–653.
- [6] A. Linke, P. Muller, D. Nurzynska, C. Casarsa, D. Torella, A. Nascimbene, C. Castaldo, S. Cascapera, M. Bohm, F. Quaini, K. Urbanek, A. Leri, T.H. Hintze, J. Kajstura, P. Anversa, Stem cells in the dog heart are self-renewing, clonogenic, and multipotent and regenerate infarcted myocardium, improving cardiac function, *Proc. Natl. Acad. Sci. USA* 102 (2005) 8966–8971.
- [7] E. Messina, L. De Angelis, G. Frati, S. Morrone, S. Chimenti, F. Fiordaliso, M. Salio, M. Battaglia, M.V. Latronico, M. Coletta, E. Vivarelli, L. Frati, G. Cossu, A. Giacomello, Isolation and expansion of adult cardiac stem cells from human and murine heart, *Circ. Res.* 95 (2004) 911–921.
- [8] K. Urbanek, F. Quaini, G. Tasca, D. Torella, C. Castaldo, B. Nadal-Ginard, A. Leri, J. Kajstura, E. Quaini, P. Anversa, Intense myocyte formation from cardiac stem cells in human cardiac hypertrophy, *Proc. Natl. Acad. Sci. USA* 100 (2003) 10440–10445.
- [9] K. Urbanek, D. Torella, F. Sheikh, A. De Angelis, D. Nurzynska, F. Silvestri, C.A. Beltrami, R. Bussani, A.P. Beltrami, F. Quaini, R. Bolli, A. Leri, J. Kajstura, P. Anversa, Myocardial regeneration by

- activation of multipotent cardiac stem cells in ischemic heart failure, *Proc. Natl. Acad. Sci. USA* 102 (2005) 8692–8697.
- [10] A.A. Mangi, N. Noiseux, D. Kong, H. He, M. Rezvani, J.S. Ingwall, V.J. Dzau, Mesenchymal stem cells modified with Akt prevent remodeling and restore performance of infarcted hearts, *Nat. Med.* 9 (2003) 1195–1201.
- [11] M. Gneocchi, H. He, N. Noiseux, O.D. Liang, L. Zhang, F. Morello, H. Mu, L.G. Melo, R.E. Pratt, J.S. Ingwall, V.J. Dzau, Evidence supporting paracrine hypothesis for Akt-modified mesenchymal stem cell-mediated cardiac protection and functional improvement, *FASEB J.* 20 (2006) 661–669.
- [12] K. Urbanek, M. Rota, S. Cascapera, C. Bearzi, A. Nascimbene, A. De Angelis, T. Hosoda, S. Chimenti, M. Baker, F. Limana, D. Nurzynska, D. Torella, F. Rotatori, R. Rastaldo, E. Musso, F. Quaini, A. Leri, J. Kajstura, P. Anversa, Cardiac stem cells possess growth factor-receptor systems that after activation regenerate the infarcted myocardium, improving ventricular function and long-term survival, *Circ. Res.* (2005).
- [13] N. Gude, J. Muraski, M. Rubio, J. Kajstura, E. Schaefer, P. Anversa, M.A. Sussman, Akt promotes increased cardiomyocyte cycling and expansion of the cardiac progenitor cell population, *Circ. Res.* 99 (2006) 381–388.
- [14] M.F. Pittenger, B.J. Martin, Mesenchymal stem cells and their potential as cardiac therapeutics, *Circ. Res.* 95 (2004) 9–20.
- [15] Y. Sakaguchi, I. Sekiya, K. Yagishita, T. Muneta, Comparison of human stem cells derived from various mesenchymal tissues: superiority of synovium as a cell source, *Arthritis Rheum.* 52 (2005) 2521–2529.
- [16] N. Kawanabe, K. Murakami, T. Takano-Yamamoto, The presence of ABCG2-dependent side population cells in human periodontal ligaments, *Biochem. Biophys. Res. Commun.* 344 (2006) 1278–1283.
- [17] H. Wang, W.K. MacNaughton, Overexpressed beta-catenin blocks nitric oxide-induced apoptosis in colonic cancer cells, *Cancer Res.* 65 (2005) 8604–8607.
- [18] D. Torella, M. Rota, D. Nurzynska, E. Musso, A. Monsen, I. Shiraishi, E. Zias, K. Walsh, A. Rosenzweig, M.A. Sussman, K. Urbanek, B. Nadal-Ginard, J. Kajstura, P. Anversa, A. Leri, Cardiac stem cell and myocyte aging, heart failure, and insulin-like growth factor-1 overexpression, *Circ. Res.* 94 (2004) 514–524.
- [19] K. Urbanek, D. Cesselli, M. Rota, A. Nascimbene, A. De Angelis, T. Hosoda, C. Bearzi, A. Boni, R. Bolli, J. Kajstura, P. Anversa, A. Leri, Stem cell niches in the adult mouse heart, *Proc. Natl. Acad. Sci. USA* 103 (2006) 9226–9231.
- [20] I.L. Weissman, Translating stem and progenitor cell biology to the clinic: barriers and opportunities, *Science* 287 (2000) 1442–1446.
- [21] L. da Silva Meirelles, P.C. Chagastelles, N.B. Nardi, Mesenchymal stem cells reside in virtually all post-natal organs and tissues, *J. Cell Sci.* 119 (2006) 2204–2213.
- [22] A. Wessels, J.M. Perez-Pomares, The epicardium and epicardially derived cells (EPDCs) as cardiac stem cells, *Anat. Rec. A Discov. Mol. Cell. Evol. Biol.* 276 (2004) 43–57.
- [23] J. van Tuyn, D.E. Atsma, E.M. Winter, I. van der Velde-van Dijke, D.A. Pijnappels, N.A. Bax, S. Knaan-Shanzer, A.C. Gittenberger-de Groot, R.E. Poelmann, A. van der Laarse, E.E. van der Wall, M.J. Schalij, A.A. de Vries, Epicardial cells of human adults can undergo an epithelial-to-mesenchymal transition and obtain characteristics of smooth muscle cells in vitro, *Stem Cells* (2006).
- [24] A.D. Sinor, L. Lillien, Akt-1 expression level regulates CNS precursors, *J. Neurosci.* 24 (2004) 8531–8541.
- [25] F.H. Bahlmann, K. De Groot, J.M. Spandau, A.L. Landry, B. Hertel, T. Duckert, S.M. Boehm, J. Menne, H. Haller, D. Fliser, Erythropoietin regulates endothelial progenitor cells, *Blood* 103 (2004) 921–926.
- [26] J. Liang, J.M. Slingerland, Multiple roles of the PI3K/PKB (Akt) pathway in cell cycle progression, *Cell Cycle* 2 (2003) 339–345.
- [27] A.S. Tseng, F.B. Engel, M.T. Keating, The GSK-3 inhibitor BIO promotes proliferation in mammalian cardiomyocytes, *Chem. Biol.* 13 (2006) 957–963.
- [28] N. Sato, L. Meijer, L. Skaltsounis, P. Greengard, A.H. Brivanlou, Maintenance of pluripotency in human and mouse embryonic stem cells through activation of Wnt signaling by a pharmacological GSK-3-specific inhibitor, *Nat. Med.* 10 (2004) 55–63.



## Skeletal myosphere-derived progenitor cell transplantation promotes neovascularization in $\delta$ -sarcoglycan knockdown cardiomyopathy

Tetsuya Nomura <sup>a,b</sup>, Eishi Ashihara <sup>a</sup>, Kento Tateishi <sup>a,b</sup>, Satoshi Asada <sup>a,b</sup>,  
Tomomi Ueyama <sup>a</sup>, Tomosaburo Takahashi <sup>a,b</sup>, Hiroaki Matsubara <sup>a,b</sup>, Hidemasa Oh <sup>a,\*</sup>

<sup>a</sup> Department of Experimental Therapeutics, Translational Research Center, Kyoto University Hospital, Kyoto 606-8507, Japan

<sup>b</sup> Department of Cardiovascular Medicine, Kyoto Prefectural University of Medicine, Kyoto 602-8566, Japan

Received 10 November 2006

Available online 27 November 2006

### Abstract

Bone marrow cells have been shown to contribute to neovascularization in ischemic hearts, whereas their impaired maturation to restore the  $\delta$ -sarcoglycan ( $\delta$ -SG) expression responsible for focal myocardial degeneration limits their utility to treat the pathogenesis of cardiomyopathy. Here, we report the isolation of multipotent progenitor cells from adult skeletal muscle, based on their ability to generate floating-myospheres. Myosphere-derived progenitor cells (MDPCs) are distinguishable from myogenic C2C12 cells and differentiate into vascular smooth muscle cells and mesenchymal progeny. The mutation in the  $\delta$ -SG has been shown to develop vascular spasm to affect sarcolemma structure causing cardiomyopathy. We originally generated  $\delta$ -SD knockdown (KD) mice and transplanted MDPCs into the hearts. MDPCs enhanced neoangiogenesis and restored  $\delta$ -SG expression in impaired vasculatures through trans-differentiation, leading to improvement of cardiac function associated with paracrine effectors secretion. We propose that MDPCs may be the promising progenitor cells in skeletal muscle to treat  $\delta$ -sarcoglycan complex mutant cardiomyopathy.

© 2006 Elsevier Inc. All rights reserved.

**Keywords:** Stem cells; Skeletal muscle; Angiogenesis;  $\delta$ -Sarcoglycan; Mesenchymal cell

Satellite cells reside beneath the basal lamina of adult skeletal muscle and mediate the postnatal growth and regeneration of muscle [1]. However, a growing number of studies are reporting the isolation of stem cells from adult skeletal muscle tissue, distinct from or descendant from satellite cells [2,3]. Multipotent skeletal muscle-derived stem cells (MDSCs) were demonstrated to be composed of a subset of a Sca-1<sup>+</sup>/CD34<sup>+</sup>/CD45<sup>-</sup> cell population [4]. These cells exhibited greater neoangiogenesis as well as regeneration of cardiomyocytes when transplanted into myocardial infarction [5] or dystrophin-deficient mdx mice [6]. Myogenic and endothelial cell progenitors were also identified in the interstitial space of

adult skeletal muscle. They were defined as a CD34<sup>+</sup>/CD45<sup>-</sup> fraction, and differentiated into vascular endothelial cells and skeletal muscle fibers after transplantation into intact skeletal muscle [7].

To take advantage of potential therapeutic opportunities, as an easily accessible tissue source for autologous transplantation, we isolated the cells from adult skeletal muscle, based on the characteristics of adult stem cells having a distinct proliferative potential to form floating-spheres, termed myospheres [8]. Myosphere-derived progenitor cells (MDPCs) expressed phenotypic characteristics resembling microvascular pericytes [9] or mesenchymal stem cells (MSCs) [10]. When introduced into ischemic hearts, MSCs were shown to prevent deleterious remodeling and to improve cardiac function [11].

Cardiomyopathy is a multifactorial disease that includes both inherited and acquired forms and is one of the most

\* Corresponding author. Fax: +81 75 751 4741.

E-mail address: [hidemasa@kuhp.kyoto-u.ac.jp](mailto:hidemasa@kuhp.kyoto-u.ac.jp) (H. Oh).

common causes of chronic heart failure. A mutation in the  $\delta$ -sarcoglycan ( $\delta$ -SG) gene was demonstrated to lead to sarcoglycan complex disruption and dystrophic changes [12]. The absence of  $\delta$ -SG specifically in vascular smooth muscle produced microinfarcts in the heart that resulted in cardiomyopathy characterized by irregularities of the coronary vasculature and focal degeneration [13]. In this study, we originally generated cardiomyopathy model by targeting  $\delta$ -SG transcripts with efficient knockdown (KD) vector pDECAP- $\delta$ -SG [14].  $\delta$ -SG KD mice showed both less vascular density and reduced  $\delta$ -SG expression in the hearts, resulted in cardiac dysfunction.

Bone marrow-derived side population (BM-SP) transplantation has been shown to engrafted into  $\delta$ -SG-deficient hearts in the absence of restoration of  $\delta$ -SG expression in cardiac muscle [15]. Therefore, the present study was designed to address the efficacy of cell therapy using MDPCs for the treatment of  $\delta$ -SG KD-induced cardiac dysfunction. Our results showed that the implanted MDPCs not only regenerated new vessels but also promoted the secretion of paracrine effectors, thereby improving cardiac function.

## Materials and methods

**MDPC isolation.** The primary hind limb muscle cells were isolated from 8-week-old C57BL/6J mice (Shimizu Laboratories Supplies) and green fluorescent protein (GFP) transgenic mice (generously donated by M. Okabe, Osaka University) using 470 U/ml collagenase type II (Worthington) for digestion. Cells were suspended in DMEM/F12 (Invitrogen) supplemented with B27, 20 ng/ml epidermal growth factor (EGF) (Sigma), and 40 ng/ml recombinant basic fibroblast growth factor (bFGF) (Promega). Cell suspensions were then cultured onto a non-coated dish at 20 cells/ $\mu$ l density over 7 days. Individual GFP<sup>+</sup> spheres were transferred onto a 24-well fibronectin-coated plate in the growth medium composed of DMEM/F12, 2% fetal bovine serum (FBS), 20 ng/ml EGF, 10 ng/ml bFGF, and 10 ng/ml leukemia inhibitory factor (LIF) (Chemicon).

**MDPC differentiation.** Culture medium was replaced by specific medium composed of DMEM, 10% FBS, 0.5 mM isobutyl-methylxanthine, and 1  $\mu$ M dexamethasone for adipogenic differentiation. Osteogenic differentiation was induced by treating cells with 250 ng/ml recombinant bone morphogenetic protein 2 (Sigma). Differentiation medium containing DMEM/F12 and 10% FBS supplemented with 10 ng/ml vascular endothelial growth factor or 50 ng/ml platelet-derived growth factor (R&D Systems) was used to induce endothelial or smooth muscle cell differentiation, respectively.

**Generation of  $\delta$ -SG KD mice.** The plasmid to express first 498-bp coding region of  $\delta$ -SG RNA was cloned by PCR using the full-length of  $\delta$ -SG cDNA (generously donated by M. Imamura, National Institute of Neuroscience, Tokyo, Japan) [16]. A plasmid expressing the 498-bp of double-stranded  $\delta$ -SG RNA was constructed into the KD vector, pDECAP (generously donated by S. Ishii, RIKEN Tsukuba Institute, Japan) [14], as an inverted repeat with a 12-bp spacer (CTCTGGTACC). The 2.2-kbp *Bgl*II–*Bam*HI fragment of pDECAP- $\delta$ -SG was released and injected into fertilized mouse oocytes.

**RNA extraction and gene expression analysis.** Total RNA was extracted using TRIzol reagent and first-strand cDNA was synthesized by SuperScript III kit (Invitrogen). Primers used were Sca-1-f: CTCTGAGGATG GACACTTCT, Sca-1-r: GGTCTGCAGGAGGACTGAGC; CD34-f: TTGACTTCTGCAACCACGGA, CD34-r: TAGATGGCAGGCTGG ACTTC; Pax7-f: GAAAGCCAAACACAGCATCGA, Pax7-r: ACCCTG ATGCATGGTTGATGG; MyoD-f: ACATAGACTTGACAGGCC

CGA, MyoD-r: AGACCTTCGATGTAGCGGATGG; Myogenin-f: TAC GTCCATCGTGGACAGCAT, Myogenin-r: TCACTAAATTCCTC GCTGG;  $\beta$ -actin-f: GCTCGTCGTCGACAACGGCTC,  $\beta$ -actin-r: CAAACATGATCTGGGTCATCTTCTC;  $\delta$ -SG-f: CCATGACCATC TGGATTCTCAAGG,  $\delta$ -SG-r: GATGGCTTCATATTGCCAGCTTC; and smooth muscle myosin heavy chain (Sm-MHC)-f: AGGAACTCC AAGCAAGTTGCAGG, Sm-MHC-r: CTGGAAGGAACAAATGAA GCCTCG. To evaluate hepatocyte growth factor (HGF) and stromal-cell-derived factor 1 (SDF-1) expression, cDNA was analyzed by kinetic real-time RT-PCR using the ABI Prism 7700 Sequence Detector system (Applied Biosystems) with Assay-on-Demand™ primer-probes sets. mRNA levels were expressed relative to an endogenous control (18S RNA).

**Fluorescence activated cell sorting (FACS) analysis.** Cells were stained with the following antibodies; FITC-conjugated antibodies against Sca-1, CD29, CD31, CD44, CD45, CD106, and CD117, PE-conjugated antibodies against CD34 and CD90 (BD Biosciences), and rat monoclonal anti-CD105 (Southern Biotechnology) followed by APC-labeled goat anti-rat IgG (BD Biosciences). Non-viable cells were stained with propidium iodide and 30,000 events were collected per sample by FACS Calibur flow cytometer (BD Biosciences). Gates were established by non-specific-Ig binding in each experiment.

**Immunofluorescence.** Specimens were fixed in 4% paraformaldehyde and stained with rat monoclonal anti-CD31 (BD Biosciences); rabbit polyclonal anti-type I collagen (LSL); mouse monoclonal antibodies against vimentin, Sm-MHC (DAKO), and  $\delta$ -SG (Novocastra). Secondary antibodies were conjugated with Alexa 488 or Alexa 555, and nuclei were visualized using 4',6-diamino-2-phenylindole (DAPI) (Invitrogen). Mouse monoclonal antibody against  $\alpha$ -smooth muscle actin ( $\alpha$ -SMA, Sigma) was conjugated with Cy3. M.O.M. Kit (Vector). Cells were labeled with 10  $\mu$ M 5-bromo-2'-deoxyuridine (BrdU) solution for 1 h in culture and BrdU detection kit (Roche) was used according to the manufacturer's instruction. Images were captured with BZ-8000 (Keyence).

**Oil red O and Alizarin red staining.** Formalin-fixed cells were stained with 0.3% oil red O (Sigma) in 60% isopropanol for 30 min at room temperature. To stain calcium deposits, cells were covered with 2% alizarin red S solution (pH 4.2, Sigma) for 3 min.

**Masson's trichrome and 5-bromo-4-chloro-3-indolyl- $\beta$ -D-galactoside (X-gal) staining.** Hearts from 28-week-old  $\delta$ -SG KD mice were fixed with 10% formalin. Paraffin-embedded hearts were sectioned and stained with Masson's trichrome. Cell-implanted hearts were fixed by perfusion with 4% paraformaldehyde, and stained with the solution composed of 1 mg/ml X-gal (Invitrogen), 5 mM K<sub>4</sub>Fe(CN)<sub>6</sub>, 5 mM K<sub>2</sub>Fe(CN)<sub>6</sub>, 2 mM MgCl<sub>2</sub>, 0.01% sodium deoxycholate, and 0.02% NP-40 for overnight.

**Retroviral transduction.** GP2-293 cells were co-transfected with the envelope vector pVSV-G and pMSCV-puro vectors using FuGENE6 (Roche). The medium supernatant was collected and centrifuged to concentrate viral stocks according to the manufacturer's instruction. MDPCs were infected with the retrovirus for 24 h, and the infected cells were selected with 2.5  $\mu$ g/ml puromycin.

**Surgical procedure.** Anesthetized 28-week-old  $\delta$ -SG KD mice ( $n = 15$ ) were intubated and positive-pressure ventilation was maintained. A half million MDPCs diluted in 20  $\mu$ l of phosphate-buffered saline (PBS) were directly transplanted into three distinct sites of myocardium. All experimental procedures and protocols using animals were approved by the Animal Care and Use Committee of Kyoto University.

**Cardiac function.** Echocardiograms were performed using SONOS 5500 and 15 MHz probe (PHILIPS). M-mode measurements of left ventricular end diastolic diameters (LVDd) were measured and used for the calculation of fractional shortening (FS) of the left ventricle (LV). As an index of LV diastolic function, transmitral early filling/atrial contraction ratio (E/A) values were determined from five independent measurements by using spectral Doppler traces.

**Statistical analysis.** All experiments were performed at least three times. Data were expressed as means  $\pm$  standard error and analyzed by one-way ANOVA with post hoc analysis. A value of  $p < 0.05$  was considered significant.

## Results

### Isolation and expansion of MDPCs

We isolated myspheres from adult skeletal muscle, based on the characteristics of adult stem cells having a distinct proliferative potential to form floating-spheres, by co-culturing the single cells from GFP transgenic and wild-type (WT) mice to exclude cell aggregation as confirmed by green mosaic fluorescence [17]. By day-7 in culture, spherical colonies composed of entirely GFP-positive or -negative cells had been formed ( $0.11 \pm 0.03\%$  of initial cells, Fig. 1A). RT-PCR demonstrated that a single mysphere was positive for Sca-1 and CD34 but lacked essential myogenic transcription factors, including Pax7, MyoD, and Myogenin, which are typically present in myogenic C2C12 cells (Fig. 1B).

For MDPC expansion, individual GFP<sup>+</sup> myspheres were transferred onto fibronectin-coated 24-well plates in the growth medium and the myspheres were allowed to attach on culture plates. Many cells migrated from the colony and were mitotically active cells as confirmed by BrdU incorporation (Fig. 1C). MDPCs continued to proliferate in the growth medium (Fig. 1D), and reached more than 120 population doublings as confirmed in three individual cell lines (Fig. 1E).

### MDPCs have mesenchymal cell-like phenotype and differentiate into endothelial and vascular smooth muscle cells

FACS analysis showed that MDPCs expressed CD29, CD44, CD90, CD105, and CD106, a typical profile for mesenchymal cells. The lack of CD31, CD45, and CD117 indicated that the cells did not include endothelial or hematopoietic progenitors. Of note, Sca-1 and CD34 were highly expressed in MDPCs (Fig. 2A). To further address their mesenchymal-cell phenotype, undifferentiated MDPCs were stained for vimentin ( $90.2 \pm 3.3\%$ , Fig. 2B) and type I collagen ( $87.4 \pm 6.9\%$ , Fig. 2C). Induction of adipogenic- and osteogenic-lineage differentiation was examined in vitro. Accumulation of lipid vacuoles was clearly visualized by oil red O staining (Fig. 2D), and Alizarin red staining detected calcium deposits in osteogenic culture (Fig. 2E), indicating that MDPCs have a mesenchymal cell-like phenotype.

To determine the angiogenic potential of MDPCs, cells were cultured under specific inductions. Immunofluorescence analysis showed that MDPCs differentiated into CD31<sup>+</sup> vasculature (Fig. 2F) and Sm-MHC<sup>+</sup> smooth muscle cells in vitro (Fig. 2G).

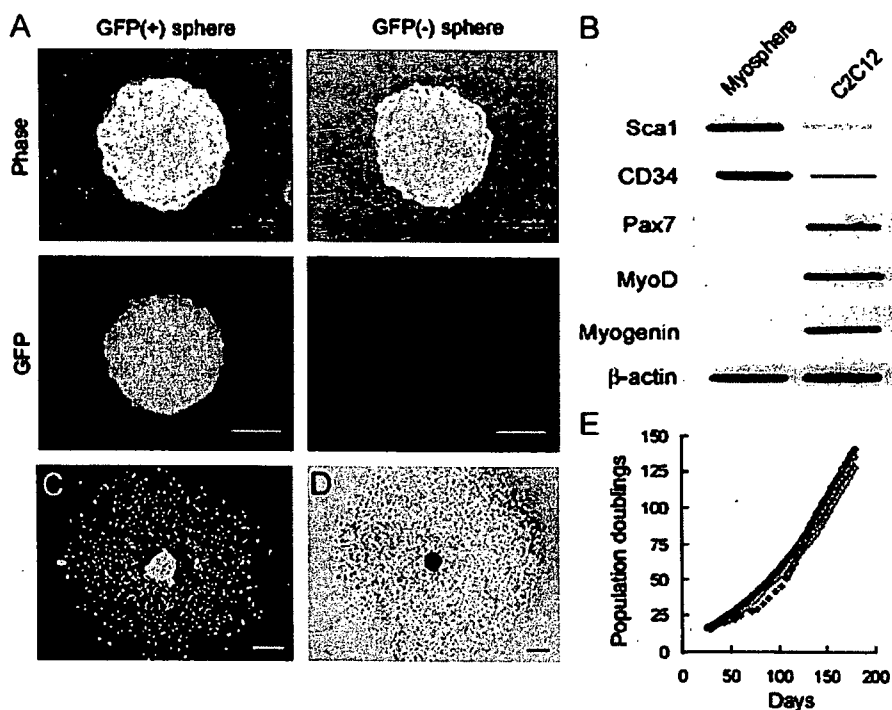


Fig. 1. Isolation and expansion of MDPCs. (A) Representative phase contrast and fluorescent images of myspheres generated from the mixed-cultures of single cells isolated from GFP transgenic (left panels) and WT mice (right panels). (B) RT-PCR analysis of Sca-1, CD34, and myogenic transcription factors. (C) MDPCs that migrated from single mysphere actively incorporated BrdU (green). DAPI (blue). (D) MDPCs propagated in the growth medium. (E) Growth kinetics of 3 independent cell lines in long-term culture. Scale bars represent 50  $\mu\text{m}$  in (C) and (D), and 20  $\mu\text{m}$  in (A).

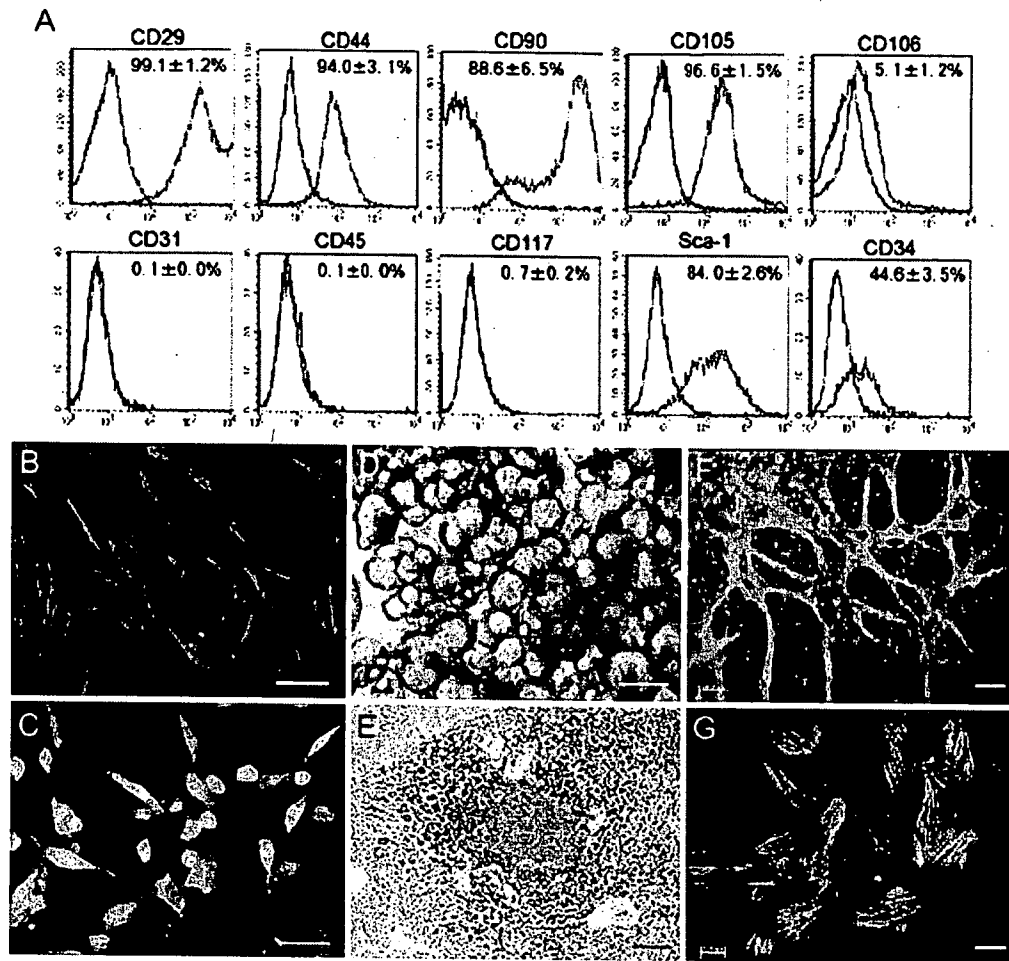


Fig. 2. MDPCs have mesenchymal cell-like phenotype and differentiate into endothelial and smooth muscle cells. (A) FACS analysis of MDPCs. Isotype controls were overlaid (blue lines) on each antigen tested (red lines). Immunostaining of mesenchymal markers on undifferentiated MDPCs. Vimentin (B, red) and type I collagen (C, green) are shown. DAPI (blue). Adipogenic- and osteogenic-inductions were verified by Oil red O (D, red) and Alizarin red (E, red), respectively. MDPCs were also induced into CD31<sup>+</sup> endothelial (F, green) and Sm-MHC<sup>+</sup> smooth muscle cells (G, red) by specific medium. DAPI (blue) Scale bars represent 50 μm in (E) and 20 μm in (B-D, F, and G).

#### MDPCs regenerate vascular smooth muscle cells with the restoration of $\delta$ -SG expression *in vivo*

We next generated  $\delta$ -SG KD mice as a cardiomyopathy model by targeting  $\delta$ -SG transcripts with an efficient KD vector, pDECAP- $\delta$ -SG [14]. Compared with non-transgenic littermates (NTG), the  $\delta$ -SG expression on the membrane of cardiac muscle was disrupted in 28-week-old  $\delta$ -SG KD mice (Fig. 3A left panels). The  $\delta$ -SG expression along the vessels was also decreased, resulting in narrow vascular lumens with constrictive morphology (Fig. 3A middle panels). Masson's trichrome staining demonstrated extensive fibrosis surrounding the vessels (Fig. 3A right panels).

To determine whether MDPC transplantation can restore the  $\delta$ -SG expression as well as regenerate the degenerated vessels in  $\delta$ -SG KD hearts, a half million MDPCs transduced with a LacZ reporter gene were directly injected into three individual sites of myocardium. All transplanted

hearts showed substantial LacZ<sup>+</sup> cell engraftment 4 weeks after implantation. LacZ<sup>+</sup> vascular smooth muscle cells could be readily detectable (Fig. 3B), and those were co-localized with  $\delta$ -SG expression to regenerate new vessels (Fig. 3C arrows).

#### Transplantation of MDPCs improves cardiac function partially through the paracrine effectors production

We next asked whether MDPCs might restore  $\delta$ -SG expression during differentiation process and found that MDPCs expressed  $\delta$ -SG transcripts through smooth muscle cell lineage induction *in vitro* (Fig. 4A). A significant neoangiogenesis in the MDPC-injected area was observed in the MDPC-transplanted group compared with that in PBS-treated hearts (Fig. 4B). Cardiac function at baseline of  $\delta$ -SG KD and NTG littermates was analyzed by echocardiography and showed a significant increase in LVDD and impaired systolic and diastolic functions in  $\delta$ -SG KD

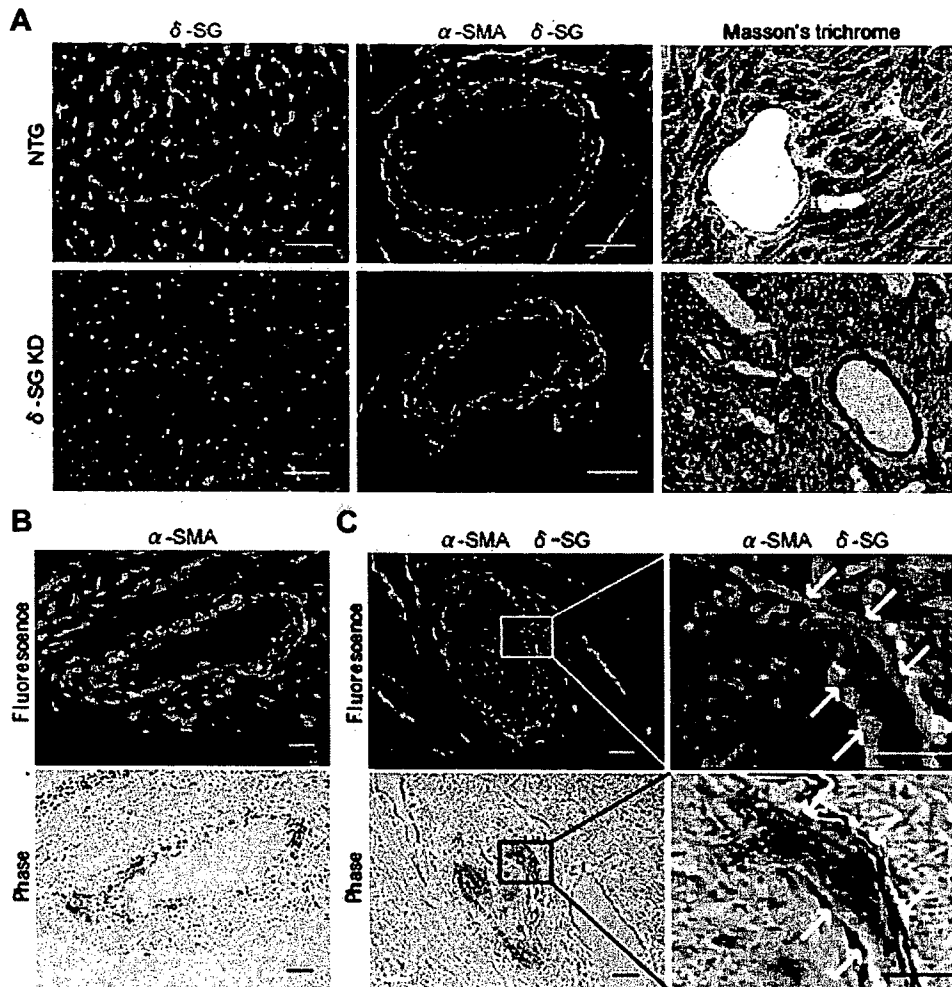


Fig. 3. Vascular regeneration in  $\delta$ -SG KD hearts with the restoration of  $\delta$ -SG expression. (A, left panels) Decreased  $\delta$ -SG (red) expression in cardiac muscle was significantly observed in  $\delta$ -SG KD hearts compared with NTG littermates. DAPI (blue). (A, middle panels) Vascular lumens were more constrictive and narrower with irregular distribution of perivascular  $\delta$ -SG expression (green) in  $\delta$ -SG KD hearts.  $\alpha$ -SMA (red). DAPI (blue). (A, right panels) Masson's trichrome staining showed perivascular fibrosis in  $\delta$ -SG KD hearts. (B) Transplanted LacZ<sup>+</sup> MDPCs differentiated into smooth muscle cells in  $\delta$ -SG KD hearts.  $\alpha$ -SMA (red) DAPI (blue). (C)  $\delta$ -SG expression (green) was restored in newly formed vessels (arrows). The right panels are magnified images of the rectangle areas in the left panels.  $\alpha$ -SMA (red) DAPI (blue). Scale bars represent 50  $\mu$ m in the left and right panels of (A), (B), and the left panels of (C), and 20  $\mu$ m in the middle panels of (A) and the right panels of (C).

hearts (Fig. 4C). Transplantation of MDPCs did not result in any significant reduction in cardiac enlargement compared with that in PBS-treated hearts, but did significantly improve LV performance 4 weeks after cell implantation (Fig. 4C). To elucidate the mechanisms of functional recovery in the MDPC-transplanted hearts, relative gene expression of paracrine mediators was measured by real-time RT-PCR. Gene expression for HGF and SDF-1 significantly increased in the MDPC-implanted hearts compared with that in the control hearts 2 weeks after cell transplantation (Fig. 4D).

## Discussion

Autologous transplantation is the ideal system of cell therapy. From this practical point of view, skeletal muscle is one of the most easily accessible tissue sources. There are

accumulating reports of multipotent progenitors in skeletal muscle, but the differentiation potential of these cells remains controversial [2]. A recent report demonstrated the isolation of myospheres from the adult skeletal muscle [8]. As opposed to the MDPCs we described here, these cells expressed Pax7 at baseline and tended to differentiate into a myogenic lineage, suggesting that these cells were originated from satellite cells. In this study, we demonstrated Pax7<sup>-</sup> MDPCs regenerated endothelial and vascular smooth muscle cells in vitro and in vivo. These MDPCs displayed prolonged self-renewal capacity, mesenchymal cell-like phenotype, and expressed part of the embryonic stem cell markers such as Nanog, Oct-4 and Sox2 (data not shown), indicative of their marked plasticity.

Although few reports to date have described the origin of skeletal muscle containing stem cell-like population, the characteristics of MDPCs shown here indicated that



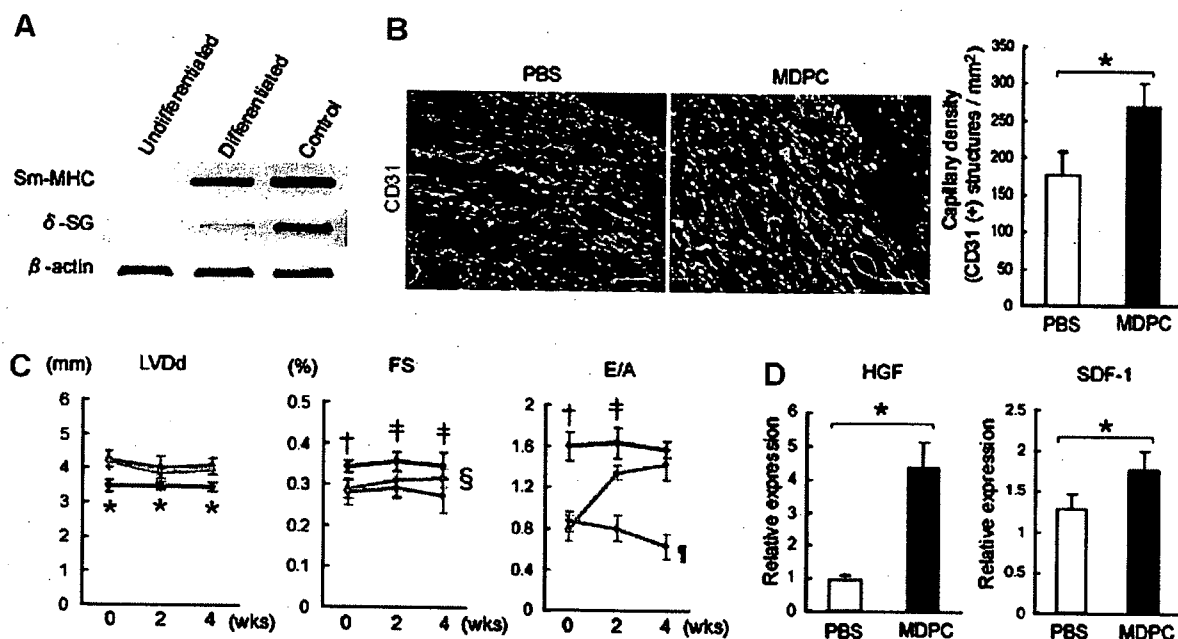


Fig. 4. MDPC transplantation improves cardiac function partially through paracrine effectors production (A)  $\delta$ -SG expression was observed in differentiated MDPCs in vitro. (B) Comparison of the capillary density between PBS-treated and MDPC-transplanted  $\delta$ -SG KD hearts. CD31 (red), DAPI (blue). \* $p < 0.01$ . (C) The effect of MDPC transplantation in  $\delta$ -SG KD hearts shown by echocardiograms. Black lines: NTG mice. Blue lines: PBS-treated group. Red lines: MDPC-transplanted group. \* $p < 0.05$ ; † $p < 0.01$  vs. PBS- and MDPC-treated mice. ‡ $p < 0.01$  vs. PBS-injected mice and § $p < 0.05$  vs. MDPC-transplanted mice. ¶ $p < 0.05$  vs. PBS-injected mice. †† $p < 0.01$  vs. NTG and MDPC-treated mice compared with the same time point. (D) Relative gene expression for HGF and SDF-1 was measured by real-time RT-PCR. \* $p < 0.01$ . Scale bars represent 50  $\mu$ m in (B).

they might be reminiscent of mesenchymal cells derived from perivascular cells (PVCs) [18] or mesoangioblasts that are putative ancestors of PVCs [19], which can be classified as pericytes in capillaries and are essential for the development of functional vessel walls. Because PVCs are thought to have the potential to regenerate mesenchymal cells, MDPCs may reflect in some aspects of the phenotype of MSCs originally isolated from bone marrow stroma.

Previous report demonstrated that BM-SP cells could be engrafted in  $\delta$ -SG null hearts, but failed to restore the  $\delta$ -SG expression [15]. The absence of  $\delta$ -SG expression after transplantation suggested that cellular fusion, as opposed to de novo differentiation, occurred with transplanted BM-SP cells which led to impaired maturation of implanted cells. In contrast, we observed that transplanted MDPCs did differentiate into mature vascular cells with the restoration of  $\delta$ -SG expression, indicating autonomous vascular-differentiation might occur after MDPC transplantation.

It is important to determine whether local intramuscular injection of MDPCs into  $\delta$ -SG KD heart is sufficient to deliver the cells into focally degenerated lesions and contributes to functional recovery. We observed extensive angiogenesis induced by MDPC transplantation to achieve a better preservation of cardiac function. However, the lack of improvement in diastolic dimension did not favor a scaffolding effect of the grafted MDPCs in  $\delta$ -SG KD hearts similar to the previous report [20]. In our study, engrafted MDPCs were incorporated mostly into vascular

cells, but muscular regeneration was rarely observed. One of the reasons is that  $\delta$ -SG KD mice showed a predominantly lower expression of  $\delta$ -SG along vascular smooth muscle cells, as previously reported [21], leading to scarce muscular artery and particularly extensive fibrosis surrounding the vessels. This focal defect in the  $\delta$ -SG KD heart might be one of the causes for transplanted MDPCs to differentiate into vascular cells more efficiently than into cardiac or skeletal muscle fibers.

Our results also suggested that transplanted MDPCs could induce the secretion of HGF and SDF-1, that is consistent with the recent reports demonstrating that HGF could promote stem cell activation and reduced cardiomyocyte apoptosis in the myocardium of  $\delta$ -SG-null hamsters [22], and that SDF-1 was sufficient to induce therapeutic stem cell homing to injured myocardium [23]. Taken together, the beneficial effects of MDPC transplantation might be due to increased blood supply produced by angiogenesis and promoted secretion of specific growth factors, leading to modulation of adverse LV remodeling and improvement of cardiac function.

In conclusion, transplantation of MDPCs induced substantial angiogenesis and increased secretion of paracrine mediators, resulting in the improvement of cardiac function in  $\delta$ -SG KD mice. Our findings indicate that MDPCs may be the promising progenitor cells in adult skeletal muscle for cell therapy to treat  $\delta$ -sarcoglycan complex mutant cardiomyopathy.

## Acknowledgments

We thank the investigators cited for generously donating plasmids: S. Ishii, and M. Imamura; Y. Yoshida, A. Kosugi, and M. Nishikawa for technical assistance. This work was supported by Grants-in-Aid from the Ministry of Education, Culture, Sports, Science and Technology of Japan, and by Grants-in-Aid from the Ministry of Health, Labor, and Welfare of Japan.

## References

- [1] C.A. Collins, I. Olsen, P.S. Zammit, L. Heslop, A. Petrie, T.A. Partridge, J.E. Morgan, Stem cell function, self-renewal, and behavioral heterogeneity of cells from the adult muscle satellite cell niche, *Cell* 122 (2005) 289–301.
- [2] I.W. McKinnell, G. Parise, M.A. Rudnicki, Muscle stem cells and regenerative myogenesis, *Curr. Top Dev. Biol.* 71 (2005) 113–130.
- [3] N. Hashimoto, T. Murase, S. Kondo, A. Okuda, M. Inagawa-Ogashiwa, Muscle reconstitution by muscle satellite cell descendants with stem cell-like properties, *Development* 131 (2004) 5481–5490.
- [4] Z. Qu-Petersen, B. Deasy, R. Jankowski, M. Ikezawa, J. Cummins, R. Pruchnic, J. Mytinger, B. Cao, C. Gates, A. Wernig, J. Huard, Identification of a novel population of muscle stem cells in mice: potential for muscle regeneration, *J. Cell Biol.* 157 (2002) 851–864.
- [5] H. Oshima, T.R. Payne, K.L. Urish, T. Sakai, Y. Ling, B. Gharaibeh, K. Tobita, B.B. Keller, J.H. Cummins, J. Huard, Differential myocardial infarct repair with muscle stem cells compared to myoblasts, *Mol. Ther.* 12 (2005) 1130–1141.
- [6] T.R. Payne, H. Oshima, T. Sakai, Y. Ling, B. Gharaibeh, J. Cummins, J. Huard, Regeneration of dystrophin-expressing myocytes in the mdx heart by skeletal muscle stem cells, *Gene Ther.* 12 (2005) 1264–1274.
- [7] T. Tamaki, A. Akatsuka, K. Ando, Y. Nakamura, H. Matsuzawa, T. Hotta, R.R. Roy, V.R. Edgerton, Identification of myogenic-endothelial progenitor cells in the interstitial spaces of skeletal muscle, *J. Cell Biol.* 157 (2002) 571–577.
- [8] R. Sarig, Z. Baruchi, O. Fuchs, U. Nudel, D. Yaffe, Regeneration and transdifferentiation potential of muscle-derived stem cells propagated as myospheres, *Stem Cells* 24 (2006) 1769–1778.
- [9] H. Gerhardt, C. Betsholtz, Endothelial-pericyte interactions in angiogenesis, *Cell Tissue Res.* 314 (2003) 15–23.
- [10] L. da Silva Meirelles, P.C. Chagastelles, N.B. Nardi, Mesenchymal stem cells reside in virtually all post-natal organs and tissues, *J. Cell Sci.* 119 (2006) 2204–2213.
- [11] M.F. Pittenger, B.J. Martin, Mesenchymal stem cells and their potential as cardiac therapeutics, *Circ. Res.* 95 (2004) 9–20.
- [12] A. Sakamoto, K. Ono, M. Abe, G. Jasmin, T. Eki, Y. Murakami, T. Masaki, T. Toyo-oka, F. Hanaoka, Both hypertrophic and dilated cardiomyopathies are caused by mutation of the same gene, delta-sarcoglycan, in hamster: an animal model of disrupted dystrophin-associated glycoprotein complex, *Proc. Natl. Acad. Sci. USA* 94 (1997) 13873–13878.
- [13] R. Coral-Vazquez, R.D. Cohn, S.A. Moore, J.A. Hill, R.M. Weiss, R.L. Davisson, V. Straub, R. Barresi, D. Bansal, R.F. Hrstka, R. Williamson, K.P. Campbell, Disruption of the sarcoglycan-sarcospan complex in vascular smooth muscle: a novel mechanism for cardiomyopathy and muscular dystrophy, *Cell* 98 (1999) 465–474.
- [14] T. Shinagawa, S. Ishii, Generation of Ski-knockdown mice by expressing a long double-strand RNA from an RNA polymerase II promoter, *Genes Dev.* 17 (2003) 1340–1345.
- [15] K.A. Lapidos, Y.E. Chen, J.U. Earley, A. Heydemann, J.M. Huber, M. Chien, A. Ma, E.M. McNally, Transplanted hematopoietic stem cells demonstrate impaired sarcoglycan expression after engraftment into cardiac and skeletal muscle, *J. Clin. Invest.* 114 (2004) 1577–1585.
- [16] S. Noguchi, E. Wakabayashi, M. Imamura, M. Yoshida, E. Ozawa, Developmental expression of sarcoglycan gene products in cultured myocytes, *Biochem. Biophys. Res. Commun.* 262 (1999) 88–93.
- [17] P. Vourc'h, M. Romero-Ramos, O. Chivatakarn, H.E. Young, P.A. Lucas, M. El-Kalay, M.F. Chesselet, Isolation and characterization of cells with neurogenic potential from adult skeletal muscle, *Biochem. Biophys. Res. Commun.* 317 (2004) 893–901.
- [18] B. Brachvogel, H. Moch, F. Pausch, U. Schlotzer-Schrehardt, C. Hofmann, R. Hallmann, K. von der Mark, T. Winkler, E. Poschl, Perivascular cells expressing annexin A5 define a novel mesenchymal stem cell-like population with the capacity to differentiate into multiple mesenchymal lineages, *Development* 132 (2005) 2657–2668.
- [19] G. Cossu, P. Bianco, Mesoangioblasts—vascular progenitors for extravascular mesodermal tissues, *Curr. Opin. Genet. Dev.* 13 (2003) 537–542.
- [20] J. Pouly, A.A. Hagege, J.T. Vilquin, A. Bissery, A. Rouche, P. Bruneval, D. Duboc, M. Desnos, M. Fiszman, Y. Fromes, P. Menasche, Does the functional efficacy of skeletal myoblast transplantation extend to nonischemic cardiomyopathy? *Circulation* 110 (2004) 1626–1631.
- [21] M.T. Wheeler, M.J. Allikian, A. Heydemann, M. Hadhazy, S. Zarnegar, E.M. McNally, Smooth muscle cell-extrinsic vascular spasm arises from cardiomyocyte degeneration in sarcoglycan-deficient cardiomyopathy, *J. Clin. Invest.* 113 (2004) 668–675.
- [22] R. Fiaccavento, F. Carotenuto, M. Minieri, C. Fantini, G. Forte, A. Carbone, L. Carosella, R. Bei, L. Masuelli, C. Palumbo, A. Modesti, M. Prat, P. Di Nardo, Stem cell activation sustains hereditary hypertrophy in hamster cardiomyopathy, *J. Pathol.* 205 (2005) 397–407.
- [23] A.T. Askari, S. Unzek, Z.B. Popovic, C.K. Goldman, F. Forudi, M. Kiedrowski, A. Rovner, S.G. Ellis, J.D. Thomas, P.E. DiCorleto, E.J. Topol, M.S. Penn, Effect of stromal-cell-derived factor 1 on stem-cell homing and tissue regeneration in ischaemic cardiomyopathy, *Lancet* 362 (2003) 697–703.



## MicroRNA-1 facilitates skeletal myogenic differentiation without affecting osteoblastic and adipogenic differentiation

Norio Nakajima <sup>a,b</sup>, Tomosaburo Takahashi <sup>a,b,\*</sup>, Ryoji Kitamura <sup>a,b</sup>, Koji Isodono <sup>a,b</sup>, Satoshi Asada <sup>a,b</sup>, Tomomi Ueyama <sup>b</sup>, Hiroaki Matsubara <sup>a,b</sup>, Hidemasa Oh <sup>b</sup>

<sup>a</sup> Department of Cardiovascular Medicine, Kyoto Prefectural University of Medicine, Kyoto 602-8566, Japan

<sup>b</sup> Department of Experimental Therapeutics, Translational Research Center, Kyoto University Hospital, Kyoto 606-8507, Japan

Received 26 September 2006  
Available online 6 October 2006

### Abstract

MicroRNAs (miRNAs) are small non-coding RNAs emerging as important post-transcriptional gene regulators. In this study, we examined the role of miR-1, an miRNA specifically expressed in cardiac and skeletal muscle tissue, on the myogenic, osteoblastic, and adipogenic differentiation of C2C12 cells. Upon induction of myogenic differentiation, miR-1 was robustly expressed. Retrovirus-mediated overexpression of miR-1 markedly enhanced expression of muscle creatine kinase, sarcomeric myosin, and  $\alpha$ -actinin, while the effects on myogenin and MyoD expression were modest. Formation of myotubes was significantly augmented in miR-1-overexpressing cells, indicating miR-1 expression enhanced not only myogenic differentiation but also maturation into myotubes. In contrast, osteoblastic and adipogenic differentiation was not affected by forced expression of miR-1. Thus, the muscle-specific miRNA, miR-1, plays important roles in controlling myogenic differentiation and maturation in lineage-committed cells, rather than functioning in fate determination.

© 2006 Elsevier Inc. All rights reserved.

**Keywords:** MicroRNA; Differentiation; Skeletal muscle cells; Adipocytes; Osteoblasts; C2C12 cells

MicroRNAs (miRNAs) are a class of small non-coding RNAs that play an important role in the post-transcriptional regulation of protein-coding gene expression. They anneal to the complementary sequences in the 3'UTRs of target mRNAs and cause degradation or, more notably, translational inhibition of target transcripts [1]. Although the functions of only a handful of miRNAs have been identified, it is emerging that miRNAs are involved in a wide variety of biological functions such as developmental patterning, lineage differentiation, cell death, proliferation, insulin secretion, and antiviral defense [2]. MiRNA-1 (miR-1) is an miRNA that is specifically expressed in cardiac and skeletal muscle [3]. Transfection of miR-1 in HeLa cells, a human epithelial cell line, has been shown to shift the gene expression profile toward that of muscle cells [4].

It has also been shown that transgenic expression of miR-1 in mouse hearts results in a proliferation defect and a failure of cardiac myocyte expansion, suggesting premature differentiation of cardiac myocytes by miR-1 overexpression [3]. A recent study revealed that miR-1 promotes myogenesis of myoblasts while repressing proliferation [5], although only relatively early steps of myoblast differentiation were examined in this study. These studies suggest that miR-1 regulates the balance between differentiation and proliferation, but the roles of miR-1 in lineage specification and terminal differentiation remain to be clarified.

The C2C12 cell line is a subclone isolated from parental C2 cells established from the regenerating thigh muscle of an adult mouse. Although C2C12 cells are widely used as a myoblast cell line, these cells are also well characterized as mesenchymal progenitor cells, and can differentiate into several mesenchymal cell types including myocytes,

\* Corresponding author. Fax: +81 75 251 5514.  
E-mail address: [ttaka@koto.kpu-m.ac.jp](mailto:ttaka@koto.kpu-m.ac.jp) (T. Takahashi).

osteoblasts, and adipocytes [6,7]. Incubation of C2C12 cells under low serum conditions induces muscle differentiation and fusion of cells into multinucleated myotubes. Treatment of C2C12 cells with bone morphogenetic protein (BMP)-2 blocks myotube formation and induces osteogenic differentiation instead [6,8,9]. Culturing the cells with adipogenic medium, treatment with long-chain fatty acids, or treatment with thiazolidinediones also blocks myotube formation and leads to typical adipocyte differentiation [7,10]. During differentiation into these cell types, the cells capture important aspects of their respective differentiation programs such as expression of tissue-specific transcription factors and functional gene products, providing unique opportunities to study the mechanisms of differentiation into these mesenchymal cell types.

Understanding the molecular mechanisms that control differentiation into various specialized types of cells is crucial not only for the advancement of stem or progenitor cell biology, but also for developing its clinical potential as a tissue regeneration therapy. Formation of specialized cells is a multistep process of specific cellular events that includes commitment into specific lineages, differentiation, and maturation. In this study, we used C2C12 cell differentiation as a model system to determine whether miR-1 plays a role in myogenic, osteoblastic, and adipogenic differentiation.

## Materials and methods

**Cell culture and differentiation induction.** C2C12 cells (a kind gift from A. Takahashi) and 3T3-L1 cells (Japanese Collection of Research Biore-sources) were maintained as described previously [11,12]. Myogenesis was induced by changing the growth medium to DMEM supplemented with 2% horse serum after the cells reached confluency [11]. Osteoblastic differentiation was induced by treating cells with 300 ng/ml recombinant human BMP-2 (Astellas Pharma) [13]. For adipogenic differentiation, the growth medium was switched to adipogenic induction medium for 3 days and subsequently to adipogenic maintenance medium for 7 days as described previously [10].

**Northern blot analysis.** Total RNA samples extracted using TRIZOL (Invitrogen) were electrophoresed on denaturing 15% polyacrylamide gels and electroblotted onto GeneScreen Plus membranes (Perkin-Elmer). The membranes were UV-crosslinked, baked, and hybridized with <sup>32</sup>P end-labeled oligonucleotide DNA probes in ULTRAhyb-Oligo (Ambion). After washing, hybridization signals were detected using the Bio-imaging analyzer system BAS5000 (Fuji Film). Mouse U6 was used as an internal control.

**Immunofluorescent microscopy and quantitative analyses of myotubes.** Cells were stained with an antibody against sarcomeric myosin (MF20; Developmental Studies Hybridoma Bank) followed by Alexa Fluor 555-conjugated anti-mouse IgG antibody (Invitrogen) with nuclear staining with DAPI. The average number of nuclei per myotube was determined by counting randomly chosen myosin-positive cells containing two or more nuclei, and 1000 nuclei per culture were counted. The fusion index was calculated as the ratio of the number of nuclei in myotubes with two or more nuclei to the total number of nuclei, and 5000 myotube nuclei were counted.

**Oil red O staining and alkaline phosphatase (ALP) assays.** Cells were fixed and stained with Oil Red O solution as described previously [12]. Oil Red O was eluted with 100% 2-propanol and measured at 490 nm absorbance for quantification. For ALP staining, cells were stained with a mixture of 0.01% (w/v) naphthol AS-MX phosphate and 0.25 mg/ml fast

violet B salt (Sigma–Aldrich) and counterstained with Mayer's Hematoxylin Solution. ALP activity was determined with *p*-nitrophenyl phosphate as a substrate.

**DNA constructs.** To express miR-1 under the control of the U6 promoter, miR-1 precursor sequences were synthesized, annealed, and ligated into the pENTR/U6 vector (Invitrogen). An miR-1 expression plasmid under the control of the long terminal repeat of PCMV virus was constructed using genomic sequences of miR1-2 containing pre-miR-1 gene sequences with 50 bp flanking each side, and the pMSCV-puro vector (Clontech). For use as a control, a pMSCV-puro vector expressing EGFP was also made.

**Retrovirus production and infection.** GP2-293 cells were cotransfected with the envelop vector pVSV-G and pMSCV-puro vectors using FuGENE6 (Roche). The medium supernatant was collected and centrifuged to concentrate virus stocks according to the manufacturer's instruction. Cells were infected with the retrovirus in the presence of 4 µg/ml polybrene for 24 h, and the infected cells were selected with 2.5 µg/ml puromycin.

**Reverse transcriptase (RT)-polymerase chain reaction (PCR).** cDNA was synthesized and analyzed by kinetic real-time PCR using the ABI Prism 7700 Sequence Detector system (Applied Biosystems) with Platinum SYBR Green qPCR SuperMix (Invitrogen). Mouse β tubulin was used for normalization, and comparative threshold (C<sub>T</sub>) method was used to assess relative abundance of the targets. Primers used were myogenin-f: TACGTCCATCGTGGACAGCAT, myogenin-r: TCAGCTAAATTCCTCGCTGG; myoD-f: ACATAGACTTGACAGGCCCGA, myoD-r: AGACCTTCGATGTAGCGGATGG; muscle creatine kinase (MCK)-f: CACCTCCACAGCACAGACAG, MCK-r: ACCTTGGCCATGTGATGTT; β-tubulin-f: GGAACATAGCCGTAAGTGC, β-tubulin-r: TCACTGTGCCTGAAGTACC; osterix-f: GGGTTAAGGGGAGCAAAGTCAGAT, osterix-r: CTGGGGAAAGGAGGCACAAAGAAG; osteocalcin-f: CTGAGTCTGACAAAGCCTTC, osteocalcin-r: GCTGTGACATCCATACTGC; ALP-f: AACCCAGACACAAGCATTCC, ALP-r: GCCTTTGAGGTTTTTGGTCA; PPARγ-f: CCTGGCAAAGCA TTTGTAT, PPARγ-r: GAAACTGGCACCCCTGAAAA; C/EBPα-f: GAACAGCAACGAGTACCGGTA, C/EBPα-r: GCCATGGCCTTGACCAAGGAG; aP2-f: CCGCAGACGACAGGA, aP2-r: CTCATGCCTTTCAAACT.

**Immunoblot analysis.** Cell lysates containing equal amounts of protein were electrophoresed on 10% SDS–polyacrylamide gels and transferred to polyvinylidene difluoride membranes (Millipore). Blots were immunoblotted with the primary antibody against sarcomeric myosin, α-actinin (EA-53; Sigma–Aldrich) or α-tubulin (Sigma–Aldrich), and horseradish peroxidase-labeled donkey anti-mouse IgG as a secondary antibody, followed by enhanced chemiluminescence (GE Healthcare) [14].

**Statistical analysis.** All experiments were performed at least three times. Data were expressed as means ± standard error and analyzed by one-way ANOVA with post hoc analysis. A value of *P* < 0.05 was considered statistically significant.

## Results and discussion

### MiR-1 is a muscle-specific miRNA that is expressed during myogenic differentiation

We first examined the expression of miR-1 in C2C12 cells during differentiation into myocytes, osteoblasts, and adipocytes. Although myotube formation was completely abolished when cells were induced to differentiate into osteoblasts, myotube formation was evident upon adipogenic differentiation (Fig. 1A). In undifferentiated cells, miR-1 was not expressed, while its expression was robustly increased when cells were induced to differentiate into myotubes, but not into osteoblasts (Fig. 1B). MiR-1 expression was also observed upon adipogenic differentiation, which

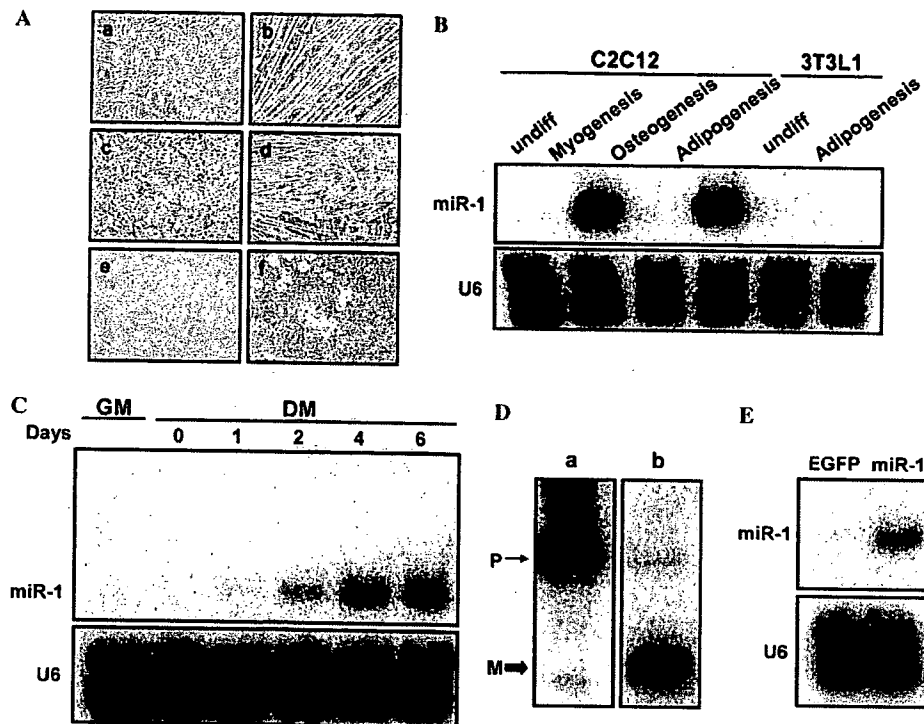


Fig. 1. MiR-1 is a muscle-specific miRNA that is expressed during myogenic differentiation. (A) Myogenic, osteoblastic, and adipogenic differentiation was induced in C2C12 cells (a–d) and 3T3-L1 cells (e,f). (a,e) Undifferentiated, (b) myogenic differentiation, (c) osteogenic differentiation, (d,f) adipogenic differentiation. (B) MiR-1 expression was analyzed in C2C12 cells or 3T3-L1 cells treated as indicated. (C) Myogenic differentiation was induced in C2C12 cells for the indicated periods of time (DM) or cells were cultured in growth medium (GM). Northern blot analysis was performed for miR-1 expression. (D) 293 cells were transfected with the pre-miR-1 (a) or the pri-miR-1-like molecule (b) expression vector, and miR-1 expression was analyzed. P, pre-miR-1; M, mature miR-1. (E) C2C12 cells were infected with EGFP or miR-1-expressing retrovirus vector, and miR-1 expression was analyzed. U6 was used as a loading control.

might reflect concomitant differentiation into myotubes in the adipogenic condition used in this study (Fig. 1A and B). MiR-1 expression was not observed in adipogenic differentiation of 3T3-L1 pre-adipocytes, where myotube formation was not observed (Fig. 1A and B). The observation that miR-1 expression was restricted to conditions that induced myotube formation was consistent with the previously observed restriction of miR-1 expression to cardiac and skeletal muscle in adult mice [3]. Kinetic analysis of miR-1 expression in myogenic differentiation revealed that miR-1 expression was readily detectable 2 days after induction of differentiation and reached its maximum at around days 4–6 (Fig. 1C). This time course correlated well with the expression of myogenic markers such as myogenin, a myogenic regulatory factor (MRF), and muscle type creatine kinase (MCK), a well-characterized marker for mature myocytes (Fig. 2), suggesting that miR-1 plays a role in controlling myogenic differentiation programs.

#### *Overexpression of miR-1 facilitates myogenic differentiation*

To analyze the role of miR-1 in C2C12 cell differentiation, we developed a vector-based expression system which efficiently expressed exogenous mature miR-1 in cells, since transient expression by synthetic RNA molecule transfection

is not suitable for stable expression during the time course of C2C12 cell differentiation. When a precursor of miR-1 (pre-miR-1) was expressed under the control of the RNA polymerase III promoter, processing from the precursor to mature miR-1 was largely impaired, as revealed by much less abundance of mature miR-1 than pre-miR-1 (Fig. 1D). We then expressed a primary miR-1 (pri-miR-1) like molecule, consisting of the pre-miR-1 plus an additional 50 nucleotides taken from its genomic sequence on each end, under the control of the RNA polymerase II promoter. With this system, efficient expression of mature miR-1 was achieved (Fig. 1D), indicating that exogenous expression of pre-miR-1 is not sufficient for entering the proper processing mechanism, whereas expression of a pri-miR-1-like molecule facilitates mature miR-1 expression. Therefore, we made a retroviral vector with this construct for efficient production of mature miR-1 in C2C12 cells (Fig. 1E).

Myogenic differentiation is a multistep dynamic process, during which the cells are defined to be myogenic (terminal commitment), differentiate into myocytes expressing muscle-specific structural and enzymatic proteins (biochemical differentiation), and subsequently fuse to form mature multinucleated myotubes (terminal differentiation). Progression through myogenic differentiation is controlled by

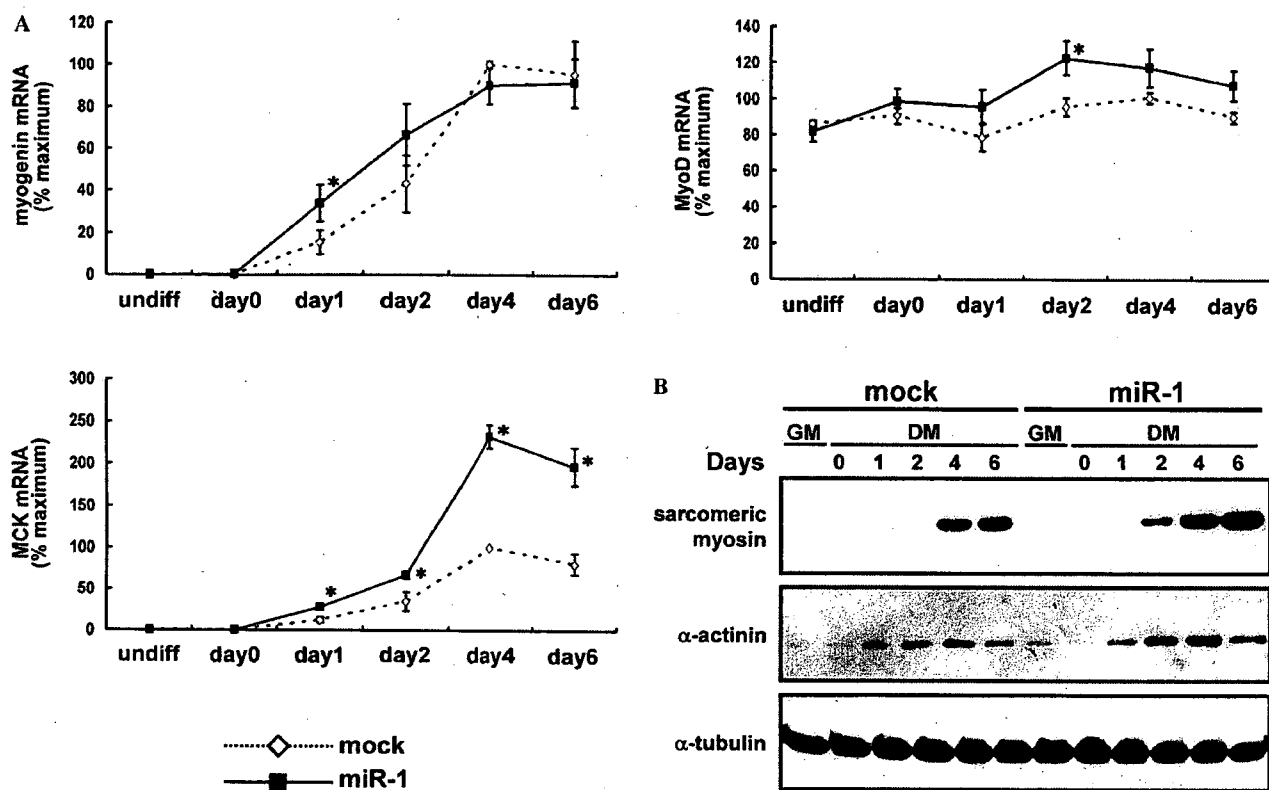


Fig. 2. Overexpression of miR-1 facilitates myogenic differentiation. Myogenic differentiation was induced for the indicated periods of time in C2C12 cells infected with mock or miR-1-expressing retrovirus. (A) Myogenin, MyoD, and MCK expression was analyzed with kinetic real-time PCR. The results were expressed as relative expression to  $\beta$ -tubulin and plotted as percentages of the maximum levels seen in mock-infected cells. \* $P < 0.05$  versus control. (B) Immunoblot analysis was performed using anti-sarcomeric myosin, anti-sarcomeric  $\alpha$ -actinin, and anti- $\alpha$ -tubulin antibodies.

sequential activation of members of muscle-specific basic helix-loop-helix proteins called MRFs [15]. Among them, MyoD is expressed in undifferentiated myoblasts, while myogenin is activated during differentiation into myocytes. Myogenin expression in miR-1-overexpressing cells was accelerated at day 1, exhibiting a 2.1-fold increase in miR-1-overexpressing cells over mock-infected cells (Fig. 2A). A recent study [5] reported a similar observation, where the effect of transfection of a synthetic miR-1 duplex on myogenin expression was evaluated up to 24 h after induction of differentiation. Later time points were then examined with the aid of retrovirus-mediated stable expression of miR-1. Myogenin expression was comparable between miR-1-overexpressing cells and control cells after day 4, and a modest increase in MyoD expression was observed by miR-1 overexpression only in the differentiating state (Fig. 2A). However, a striking increase was observed in MCK expression in miR-1-overexpressing cells compared to mock-infected cells in the late phase (Fig. 2A). About a 2.7- and 3.8-fold enhancement in MCK expression in miR-1 cells was observed at day 4 and 6, respectively. Western blot analysis with anti-sarcomeric myosin and anti-sarcomeric  $\alpha$ -actinin antibodies revealed that expression of these structural proteins was not only accelerated but also augmented by miR-1 overexpression (Fig. 2B).

These results indicated that miR-1 overexpression enhanced the biochemical differentiation of myocytes.

#### *MiR-1 overexpression leads to enhanced formation of multinucleated mature myotubes*

Fusion of individual myocytes to form multinucleated mature myotubes is a unique feature of skeletal myogenic differentiation, and myoblast fusion has been shown to be regulated by mechanisms genetically dissociated from other myogenic processes such as biochemical differentiation [16–19]. Therefore, we analyzed the effect of miR-1 expression on the formation of mature myotubes and observed that in miR-1-overexpressing cells, myotubes were both higher in number and larger in size compared to mock-infected cells (Fig. 3A). This observation was quantified by the average number of nuclei per myotube (Fig. 3B), and by the percentage of all nuclei present in myotubes (fusion index) [20] (Fig. 3C). The results showed about a 1.9-fold increase in nuclei per myotube and a 1.6-fold increase in the fusion index.

Taken together, these results indicate that in addition to its role in the early steps of myogenic differentiation [5], miR-1 also plays an important role in late biochemical differentiation and in terminal differentiation. This was

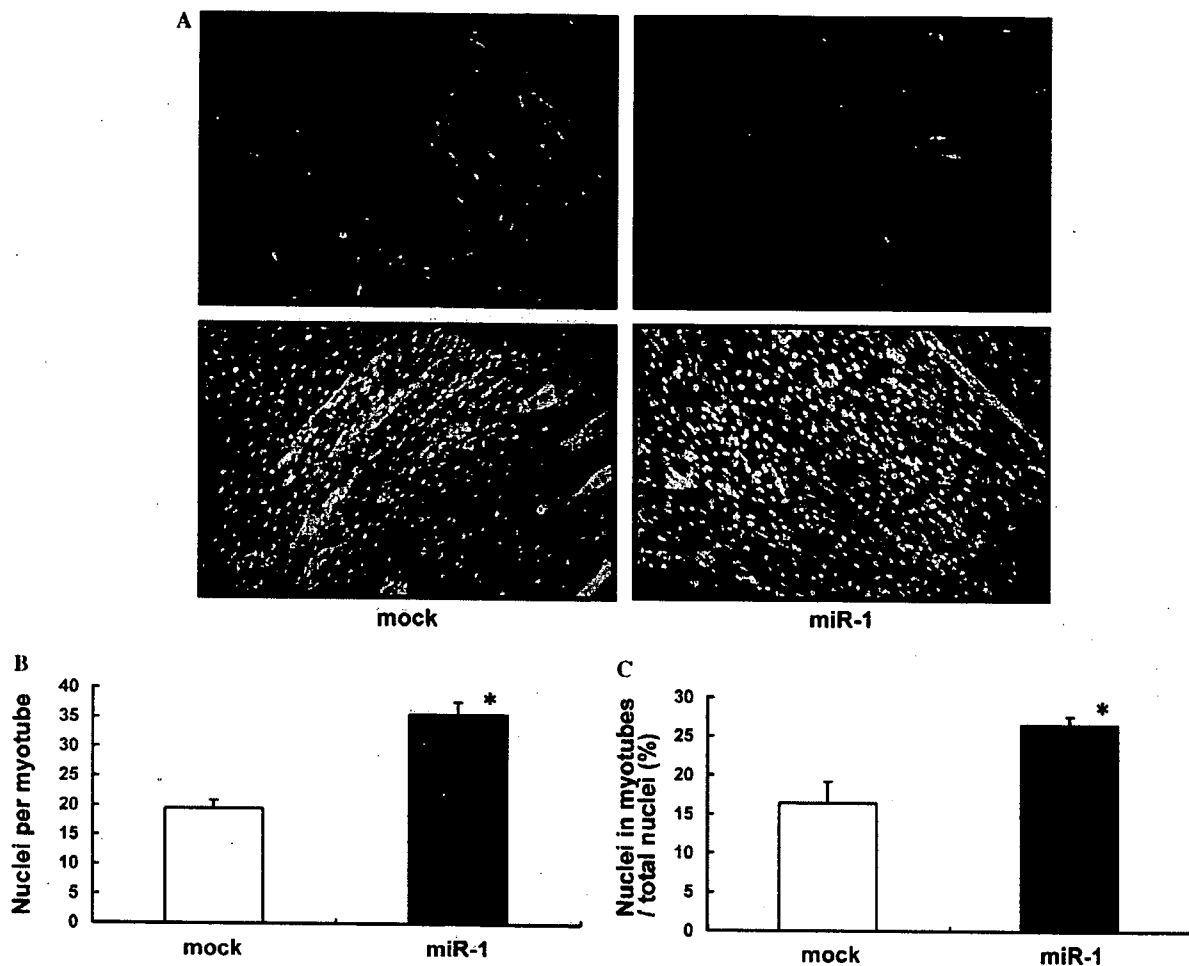


Fig. 3. MiR-1 overexpression leads to enhanced formation of multinucleated mature myotubes. Cells infected with mock or miR-1-expressing retrovirus were induced for myogenic differentiation for 6 days. (A) Myotubes were stained with anti-sarcomeric myosin antibody, and nuclei were stained with DAPI. (B) The mean number of nuclei per myotube was determined by counting 1000 nuclei per culture in three independent cultures. (C) The fusion index was defined as the ratio of nuclei within myotubes (cells containing two or more nuclei) to total number of nuclei, and percentages were plotted. Five thousand nuclei per culture were counted in three independent cultures. \* $P < 0.05$  versus control.

supported by: (i) the similar kinetics of endogenous miR-1 expression (Fig. 1C) with the expression of MCK, sarcomeric myosin, and  $\alpha$ -actinin (Fig. 2A and B), and the formation of myotubes, which all peaked at days 4–6 after induction; and (ii) the enhancement of expression of mature myocyte markers and myotube fusion with overexpression of miR-1.

In the heart, which also endogenously expresses miR-1, it has been reported that overexpression of miR-1 in mouse hearts leads to a decrease in proliferating ventricular cardiac myocytes [3]. Although the role of miR-1 in the determination of myocyte fate could not be evaluated in this study, as a cardiac-specific  $\beta$ -myosin heavy chain promoter was used to drive miR-1 expression in cardiac myocytes, these results suggest that miR-1 expression in cardiac myocytes results in enhanced or premature differentiation of cardiac myocytes that impairs the balance between differentiation and proliferation. CHIP assays have demonstrated that MyoD and myogenin bind to regions upstream to miR-1

genes, suggesting these MRFs regulate expression of miR-1 [21]. These results with our observations suggested that miR-1 plays an important role in the relatively late stages of myogenic differentiation, although further studies are needed to fully clarify the functions of miR-1 in myogenesis.

#### *MiR-1 does not influence osteoblastic or adipogenic differentiation*

Since it is not known whether miR-1 plays a role in specification of cell fate to myogenic lineages, we analyzed the effects of miR-1 overexpression on the osteoblastic and adipogenic differentiation of C2C12 cells. The osteoblastic and adipogenic differentiation programs are also multistep processes [10,12,22,23], so we evaluated the expression of transcription factors involved in determination and initial differentiation of these lineages such as osterix, PPAR $\gamma$ , and C/EBP $\alpha$ , relatively late differentiation markers such

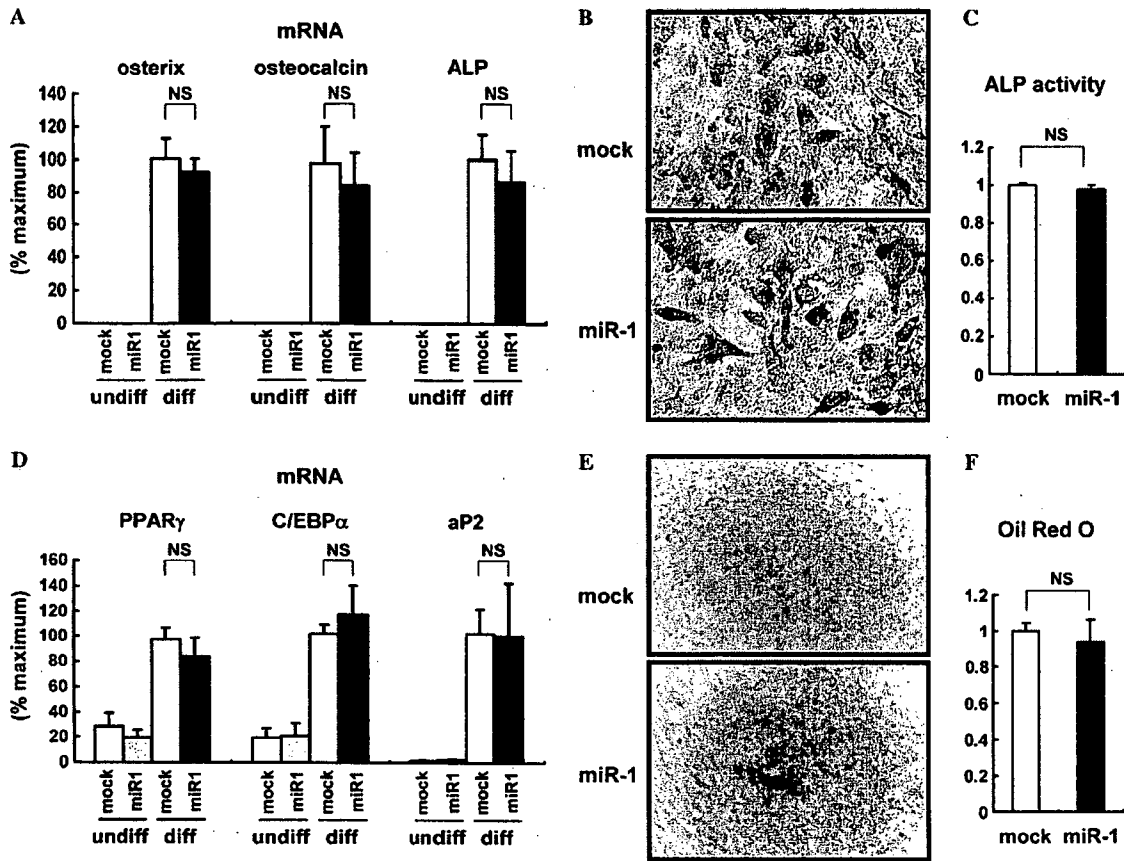


Fig. 4. MiR-1 does not influence osteoblastic or adipogenic differentiation. Osteoblastic (A–C) or adipogenic (D–F) differentiation was induced in mock-infected and miR-1-overexpressing C2C12 cells. (A) Osterix, osteocalcin, and ALP expression was measured by kinetic real-time PCR in undifferentiated and differentiated cells. (B) ALP staining was performed in differentiated cells. (C) ALP activity was determined with *p*-nitrophenyl phosphate as a substrate. (D) Kinetic PCR analysis was performed to analyze expression of PPAR $\gamma$ , C/EBP $\alpha$ , and aP2 in undifferentiated and differentiated cells. (E) Differentiated cells were stained with Oil Red O. (F) To quantify lipid accumulation, Oil Red O was extracted, and optical density was measured at 490 nm. NS; not significant.

as osteocalcin, ALP, and aP2, and characteristic biochemical features of these cells such as ALP activity and lipid accumulation. The osteoblastic markers osterix, osteocalcin, and ALP were absent in undifferentiated C2C12 cells, but markedly induced upon induction of osteoblastic differentiation (Fig. 4A). Neither the expression of these osteoblastic markers nor ALP staining and activity was altered by the exogenous expression of miR-1 during osteoblastic differentiation (Fig. 4A–C). When cells were cultured in adipogenic condition, adipogenic markers such as PPAR $\gamma$ , C/EBP $\alpha$ , and aP2 and lipid accumulation were significantly induced, and the forced expression of miR-1 did not alter the expression of these adipogenic marker genes or lipid accumulation in the cells (Fig. 4D–F). It has been reported that exogenous miR-1 expression in non-muscle cells shifts the mRNA expression profile towards muscle by downregulating the expression of genes not expressed in muscle [4]. Although these results suggested that miR-1 might act to prevent cells from differentiating into lineages other than muscle, our results showed

that osteoblastic and adipogenic differentiation was not modulated by the expression of miR-1, implying that miR-1 does not function in determination of cell fate.

### Conclusion

In this study, we analyzed the role of miR-1 in myogenic, osteoblastic, and adipogenic differentiation of C2C12 cells, and found that miR-1 enhanced myogenic differentiation and maturation into myotubes, but did not affect osteoblastic and adipogenic differentiation. These results suggest that miR-1 plays important roles in controlling the myogenic differentiation and maturation in lineage-committed cells, rather than functioning in fate determination. Identification of downstream targets of miR-1 will be an important issue to fully clarify the roles of miR-1 in myogenesis, which could be coordinately regulated by multiple miR-1 targets, since bioinformatic predictions indicate that each miRNA regulates on average ~200 target transcripts [24].



## Acknowledgments

We thank Akihiro Takahashi for providing C2C12 cells, Astellas Pharma for BMP-2, Parth Patwari for critical reading of the manuscript, and Atsumi Kosugi and Mami Nishikawa for expert technical assistance. This work was supported by Grants-in-Aid from the Ministry of Education, Culture, Sports, Science and Technology of Japan, a grant from the Mitsubishi Pharma Research Foundation and Grants-in-Aid from the Ministry of Health, Labor, and Welfare of Japan.

## References

- [1] P.H. Olsen, V. Ambros, The *lin-4* regulatory RNA controls developmental timing in *Caenorhabditis elegans* by blocking LIN-14 protein synthesis after the initiation of translation, *Dev. Biol.* 216 (1999) 671–680.
- [2] E. Wienholds, R.H.A. Plasterk, MicroRNA function in animal development, *FEBS Lett.* 579 (2005) 5911–5922.
- [3] Y. Zhao, E. Samal, D. Srivastava, Serum response factor regulates a muscle-specific microRNA that targets *Hand2* during cardiogenesis, *Nature* 436 (2005) 214–220.
- [4] L.P. Lim, N.C. Lau, P. Garrett-Engle, A. Grimson, J.M. Schelter, J. Castle, D.P. Bartel, P.S. Linsley, J.M. Johnson, Microarray analysis shows that some microRNAs downregulate large numbers of target mRNAs, *Nature* 433 (2005) 769–773.
- [5] J.F. Chen, E.M. Mandel, J.M. Thomson, Q. Wu, T.E. Callis, S.M. Hammond, F.L. Conlon, D.Z. Wang, The role of microRNA-1 and microRNA-133 in skeletal muscle proliferation and differentiation, *Nat. Genet.* 38 (2006) 228–233.
- [6] T. Katagiri, A. Yamaguchi, M. Komaki, E. Abe, N. Takahashi, T. Ikeda, V. Rosen, J.M. Wozney, A. Fujisawa-Sehara, T. Suda, Bone morphogenetic protein-2 converts the differentiation pathway of C2C12 myoblasts into the osteoblast lineage, *J. Cell Biol.* 127 (1994) 1755–1766.
- [7] L. Teboul, D. Gaillard, L. Staccini, H. Inadera, E.Z. Amri, P.A. Grimaldi, Thiazolidinediones and fatty acids convert myogenic cells into adipose-like cells, *J. Biol. Chem.* 270 (1995) 28183–28187.
- [8] E. Chalaux, T. Lopez-Rovira, J.L. Rosa, R. Bartrons, F. Ventura, JunB is involved in the inhibition of myogenic differentiation by bone morphogenetic protein-2, *J. Biol. Chem.* 273 (1998) 537–543.
- [9] D.S. de Jong, W.T. Steegenga, J.M. Hendriks, E.J. van Zoelen, W. Olijve, K.J. Dechering, Regulation of Notch signaling genes during BMP2-induced differentiation of osteoblast precursor cells, *Biochem. Biophys. Res. Commun.* 320 (2004) 100–107.
- [10] T. Akimoto, T. Ushida, S. Miyaki, H. Akaogi, K. Tsuchiya, Z. Yan, R.S. Williams, T. Tateishi, Mechanical stretch inhibits myoblast-to-adipocyte differentiation through Wnt signaling, *Biochem. Biophys. Res. Commun.* 329 (2005) 381–385.
- [11] A. Takahashi, Y. Kureishi, J. Yang, Z. Luo, K. Guo, D. Mukhopadhyay, Y. Ivashchenko, D. Branellec, K. Walsh, Myogenic Akt signaling regulates blood vessel recruitment during myofiber growth, *Mol. Cell. Biol.* 22 (2002) 4803–4814.
- [12] J.B. Hansen, R.K. Petersen, B.M. Larsen, J. Bartkova, J. Alsner, K. Kristiansen, Activation of peroxisome proliferator-activated receptor  $\gamma$  bypasses the function of the retinoblastoma protein in adipocyte differentiation, *J. Biol. Chem.* 274 (1999) 2386–2393.
- [13] Y. Lee, C. Ahn, J. Han, H. Choi, J. Kim, J. Yim, J. Lee, P. Provost, O. Radmark, S. Kim, V.N. Kim, The nuclear RNase III Drosha initiates microRNA processing, *Nature* 425 (2003) 415–419.
- [14] T. Takahashi, B. Lord, P.C. Schulze, R.M. Fryer, S.S. Sarang, S.R. Gullans, R.T. Lee, Ascorbic acid enhances differentiation of embryonic stem cells into cardiac myocytes, *Circulation* 107 (2003) 1912–1916.
- [15] M. Buckingham, L. Bajard, T. Chang, P. Daubas, J. Hadchouel, S. Meilhac, D. Montarras, D. Rocancourt, F. Relaix, The formation of skeletal muscle: from somite to limb, *J. Anat.* 202 (2003) 59–68.
- [16] M. Crescenzi, D.H. Crouch, F. Tato, Transformation by myc prevents fusion but not biochemical differentiation of C2C12 myoblasts: mechanisms of phenotypic correction in mixed culture with normal cells, *J. Cell Biol.* 125 (1994) 1137–1145.
- [17] S. Russo, D. Tomatis, G. Collo, G. Tarone, F. Tato, Myogenic conversion of NIH3T3 cells by exogenous MyoD family members: dissociation of terminal differentiation from myotube formation, *J. Cell Sci.* 111 (1998) 691–700.
- [18] I.H. Park, J. Chen, Mammalian target of rapamycin (mTOR) signaling is required for a late-stage fusion process during skeletal myotube maturation, *J. Biol. Chem.* 280 (2005) 32009–32017.
- [19] A. Piscoconti, S. Brunelli, M. Di Padova, C. De Palma, D. Deponti, S. Baesso, V. Sartorelli, G. Cossu, E. Clementi, Follistatin induction by nitric oxide through cyclic GMP: a tightly regulated signaling pathway that controls myoblast fusion, *J. Cell Biol.* 172 (2006) 233–244.
- [20] V. Jacquemin, D. Furling, A. Bigot, G.S. Butler-Browne, V. Mouly, IGF-1 induces human myotube hypertrophy by increasing cell recruitment, *Exp. Cell Res.* 299 (2004) 148–158.
- [21] P.K. Rao, R.M. Kumar, M. Farkhondeh, S. Baskerville, H.F. Lodish, Myogenic factors that regulate expression of muscle-specific microRNAs, *Proc. Natl. Acad. Sci. USA* 103 (2006) 8721–8726.
- [22] A. Nakashima, T. Katagiri, M. Tamura, Cross-talk between Wnt and bone morphogenetic protein 2 (BMP-2) signaling in differentiation pathway of C2C12 myoblasts, *J. Biol. Chem.* 280 (2005) 37660–37668.
- [23] Y.J. Kim, M.H. Lee, J.M. Wozney, J.Y. Cho, H.M. Ryoo, Bone morphogenetic protein-2-induced alkaline phosphatase expression is stimulated by Dlx5 and repressed by Msx2, *J. Biol. Chem.* 279 (2004) 50773–50780.
- [24] A. Krek, D. Grun, M.N. Poy, R. Wolf, L. Rosenberg, E.J. Epstein, P. MacMenamin, I. da Piedade, K.C. Gunsalus, M. Stoffel, N. Rajewsky, Combinatorial microRNA target predictions, *Nat. Genet.* 37 (2005) 495–500.

# Glia Maturation Factor- $\gamma$ Is Preferentially Expressed in Microvascular Endothelial and Inflammatory Cells and Modulates Actin Cytoskeleton Reorganization

Koji Ikeda, Ramendra K. Kundu, Shoko Ikeda, Miyuki Kobara,  
Hiroaki Matsubara, Thomas Quertermous

**Abstract**—Actin cytoskeleton reorganization is a fundamental process for actin-based cellular functions such as cytokinesis, phagocytosis, and chemotaxis. Regulating actin cytoskeleton reorganization is therefore an attractive approach to control endothelial and inflammatory cells function and to treat cardiovascular diseases. Here, we identified glia maturation factor- $\gamma$  (GMFG) as a novel factor in actin cytoskeleton reorganization and is expressed preferentially in microvascular endothelial and inflammatory cells. During mouse embryogenesis, GMFG was expressed predominantly in blood islands of the yolk sac, where endothelial and hematopoietic cells develop simultaneously. In endothelial cells, GMFG was colocalized with F-actin in membrane ruffles and was associated with F-actin assessed by actin co-sedimentation assay. Interestingly, GMFG was phosphorylated at N-terminal serine, and its phosphorylation was enhanced by coexpression of dominant active Rac1 and Cdc42. Furthermore, a pseudophosphorylated form of GMFG (GMFG-S2E) demonstrated higher association with F-actin. Stable expression of GMFG-S2E remarkably enhanced stimulus-responsive lamellipodia and subsequent membrane ruffle formation in HeLa cells presumably through its interaction with Arp2/3 complex. Expression of GMFG enhanced actin-based cellular functions such as migration and tube-formation in endothelial cells. Moreover, we found that GMFG expression was significantly increased in a cardiac ischemia/reperfusion model where inflammation and angiogenesis take place actively. Taken together, our findings define a novel pathway in the regulation of actin-based cellular functions. Regulating GMFG function may provide a novel approach to modulate the pathophysiology of cardiovascular diseases. (*Circ Res.* 2006;99:424-433.)

**Key Words:** actin cytoskeleton reorganization ■ actin-based cellular function  
■ microvascular endothelial cells ■ inflammatory cells

Endothelial cells, composing a single layer inside the blood vessels, play critical roles in a variety of physiological and pathological phenomena such as angiogenesis and atherosclerosis. Because genes specifically or preferentially expressed in endothelial cells are likely to play a crucial role for their unique physiology, we performed a series of microarray studies aimed at isolating unique endothelial cell genes. We successfully identified several genes specifically or preferentially expressed in endothelial cells.<sup>1</sup> Among these genes, glia maturation factor- $\gamma$  (GMFG) demonstrated a very unique expression pattern: expressed only in microvascular endothelial cells but not by endothelial cells from other vascular beds or nonendothelial cells. These results urged us to further analyze GMFG function in endothelial cells.

GMFG was initially identified as a molecule that was highly similar to glia maturation factor- $\beta$ .<sup>2</sup> However, GMFG is expressed neither in brain, neuronal cells, nor glia cells, and

its function is entirely unknown. We found the amino acid sequence of GMFG is similar to cofilin, a key regulator of actin cytoskeleton reorganization and thus analyzed GMFG function in actin cytoskeleton reorganization. Actin cytoskeleton reorganization is clearly an essential factor for a large number of cellular processes such as cytokinesis, endocytosis, and chemotaxis.<sup>3,4</sup> In response to extracellular stimuli, motile protrusions of plasma membrane, called lamellipodia or filopodia are created by the continuous polarized growth and turnover of actin filaments, leading to actin-based cellular functions.<sup>3,4</sup> Deficient actin cytoskeleton reorganization causes impaired endothelial cell migration, reduces macrophage phagocytosis, and results in defective lymphocyte development and activation.<sup>5-7</sup> Actin cytoskeleton reorganization is thus pivotal for angiogenesis and immune system function.

Actin dynamics is regulated by an elaborate mechanism that involves many actin-associated molecules. In resting

Original received March 26, 2006; revision received July 12, 2006; accepted July 13, 2006.

From the Donald W. Reynolds Cardiovascular Clinical Research Center (K.I., R.K.K., T.Q.), Division of Cardiovascular Medicine, Stanford University School of Medicine, Calif; Department of Clinical Pharmacology (M.K.), Kyoto Pharmaceutical University, Japan; and Department of Cardiology and Vascular Regenerative Medicine (K.I., S.I., H.M.), Kyoto Prefectural University of Medicine, Japan.

Correspondence to Koji Ikeda, Department of Cardiology and Vascular Regenerative Medicine, Kyoto Prefectural University of Medicine, Kyoto, Kawaramachi-Hirokoji, Kamigyo-ku, Kyoto 602-8566, Japan. E-mail ikedak@koto.kpu-m.ac.jp

© 2006 American Heart Association, Inc.

*Circulation Research* is available at <http://circres.ahajournals.org>

DOI: 10.1161/01.RES.0000237662.23539.0b

cells, actin monomers are kept from polymerizing by monomer-binding protein such as thymosin- $\beta$ 4, twinfilin, and profilin.<sup>3,8</sup> Capping proteins such as CapZ and gelsolin are also required to maintain a pool of actin monomers by capping free barbed ends of actin filaments, resulting in blocking the addition of actin monomers to the barbed ends. Extracellular stimuli activate Wiscott-Aldrich syndrome protein (WASP) and WASP family verprolin homologous (WAVE) largely through small GTPases, Rac, and Cdc42. Activated WASP/WAVE further activates the actin-related protein 2/3 (Arp2/3) complex to nucleate actin polymerization by serving as a template for the formation of new actin filaments.<sup>3</sup> During the active actin polymerization at the barbed ends, actin-depolymerization takes place as a result of the function of cofilin at the pointed ends, which replenishes the actin monomer pool.<sup>4,9,10</sup>

Recently, it has been reported that WAVE2 is expressed predominantly in endothelial cells during embryogenesis and that its deficiency causes embryonic lethality because of hemorrhage.<sup>5</sup> WAVE2<sup>-/-</sup> mice demonstrated decreased sprouting and branching of endothelial cells from existing vessels during angiogenesis. Furthermore, the formation of lamellipodia and capillaries was severely impaired in WAVE2<sup>-/-</sup> endothelial cells. These results indicate that proper regulation of actin cytoskeleton reorganization is critical for endothelial cell migration and angiogenesis.

Here, we report the characterization of GMFG, a novel factor in actin cytoskeleton reorganization, preferentially expressed in microvascular endothelial cells and inflammatory cells. GMFG remarkably enhanced stimulus-responsive lamellipodia formation, and its function was likely regulated via phosphorylation of N-terminal serine under the control of small GTPases. Overexpression of GMFG enhanced actin-based cellular functions such as cell motility and tube-formation in endothelial cells. Regulating GMFG function may provide a unique opportunity to control actin cytoskeleton reorganization in microvascular endothelial and inflammatory cells and, therefore, to modulate the pathophysiology of ischemic and inflammatory diseases.

## Materials and Methods

### DNA Constructs

Full-length human GMFG and cofilin were obtained by RT-PCR using cDNA prepared from human microvascular endothelial cells. A *Bam*HI site was created before the stop codon by adding 5'-GGATCC-3' at the beginning of reverse primer. Mutagenesis was performed by creating point mutations in the forward primers that cause a missense mutation of serine into alanine or glutamic acid. These cDNAs were subcloned into pCR-blunt II-TOPO vector (Invitrogen) and the nucleotide sequence was validated. Fragments cut out with *Eco*RI and *Bam*HI were subcloned into p3XFLAG-CMV-14 expression vector (Sigma) to obtain the expression constructs.

### Reverse-Transcription PCR

Total RNA was isolated from cells cultured in growth media, followed by cDNA synthesis. Primers used for GMFG amplification were of 100% match for both human and bovine GMFG, 5'-GACTCCCTGGTGGTGTG-3' and 5'-TACAACGAAAGAAAGACAACCTT-3'. Twenty-eight PCR cycles with annealing temperature at 57°C were performed for amplification of both GMFG and GAPDH.

### In Situ Hybridization

Whole-mount in situ hybridization was performed using digoxigenin-labeled cRNA as previously described.<sup>11</sup> After all procedures, embryos were embedded in OCT and snap-frozen by immersion in ethanol cooled on dry ice. Sections were counterstained with eosin.

### Transfection and Immunofluorescence Study

Expression constructs were transfected into bovine aortic endothelial cells (BAECs) or HeLa cells using Lipofectamine 2000 (Invitrogen) according to the recommendations of the manufacturer. Cells were plated into chamber slides 24 hours after transfection and further incubated for 24 hours followed by staining with Alexa Fluor3-phalloidin (Molecular Probes) and FITC-anti-FLAG M2 antibody (Sigma). After mounting, cells were observed under a fluorescent microscope (Axioplan 2; Zeiss).

### Cell Culture

BAECs in passage 4 to 7 were used for all experiments. Human microvascular endothelial cells were obtained from Clonetics and cultured in EGM-2MV media. To generate stable transfectants, HeLa cells underwent the selection in the growth media containing 300  $\mu$ g/mL G418, and pooled clones were used for experiments. Expression of transgenes was confirmed by RT-PCR using vector-specific primers, 5'-AAGCTTGGCCGCGAATTC-3' and 5'-TTTGTAGTCAGCCCGGATCC. The nucleotide sequence of the PCR product was validated by direct sequencing. Recombinant protein expression was confirmed by immunoblotting using anti-FLAG M2 antibody (Stratagene). For epidermal growth factor (EGF) stimulation experiment, HeLa cells were cultured in serum-free media for 24 hours, followed by stimulation with 100 ng/mL or 1000 ng/mL EGF (Sigma) for 5 minutes. Cells were fixed with 4% paraformaldehyde and observed under a phase-contrast microscope (TE 2000 U; Nikon).

### Metabolic Labeling

Cells were labeled by incubating with 1 mCi/mL of P<sup>32</sup>-phosphate (Perkin Elmer) in phosphate-free DMEM containing 10% dialyzed FBS (Invitrogen) for 4 hours. Immunoprecipitated recombinant proteins were run on SDS-PAGE and then transferred onto polyvinylidene difluoride (PVDF) membrane. Phosphorylated proteins were visualized by autoradiography.

### Actin Co-Sedimentation Assay

BAECs transiently transfected with cofilin or GMFG were collected in ice-cold PBS and resuspended in binding buffer (10 mmol/L imidazole, pH 7.2, 75 mmol/L KCl, 5 mmol/L MgCl<sub>2</sub>, 1 mmol/L EGTA, 0.5 mmol/L dithiothreitol [DTT], 0.2 mmol/L ATP, 1 mmol/L NaF, 0.5 mmol/L Na<sub>3</sub>VO<sub>4</sub>, and protease inhibitor cocktail). Nonmuscle actin was obtained from Cytoskeleton Inc and polymerized according to the instructions of the manufacturer. Cell lysates were prepared with three bursts of sonication followed by ultracentrifugation at 150 000g, and then the supernatants were incubated in the presence or absence of 5.5  $\mu$ mol/L F-actin at room temperature for 30 minutes. The reaction mixtures underwent ultracentrifuge at 150 000g for 30 minutes to precipitate F-actin. Supernatants were carefully collected and pellets were resuspended in exactly the same volume of binding buffer as the supernatants. Proteins of interest were detected by immunoblotting, and the amount of sedimentation was assessed by densitometry analysis.

### Modified Boyden Chamber Assay and Two-Dimensional Tube-Formation Assay

Modified Boyden chamber assay and tube-formation assay were performed as previously described.<sup>12</sup>

### Arp2/3 Complex-Binding Assay

Arp 2/3 complex in cell lysates was immunoprecipitated with anti-ARPC2 antibody (Upstate). Coprecipitation of GMFG was detected by immunoblotting using anti-FLAG M2 antibody.

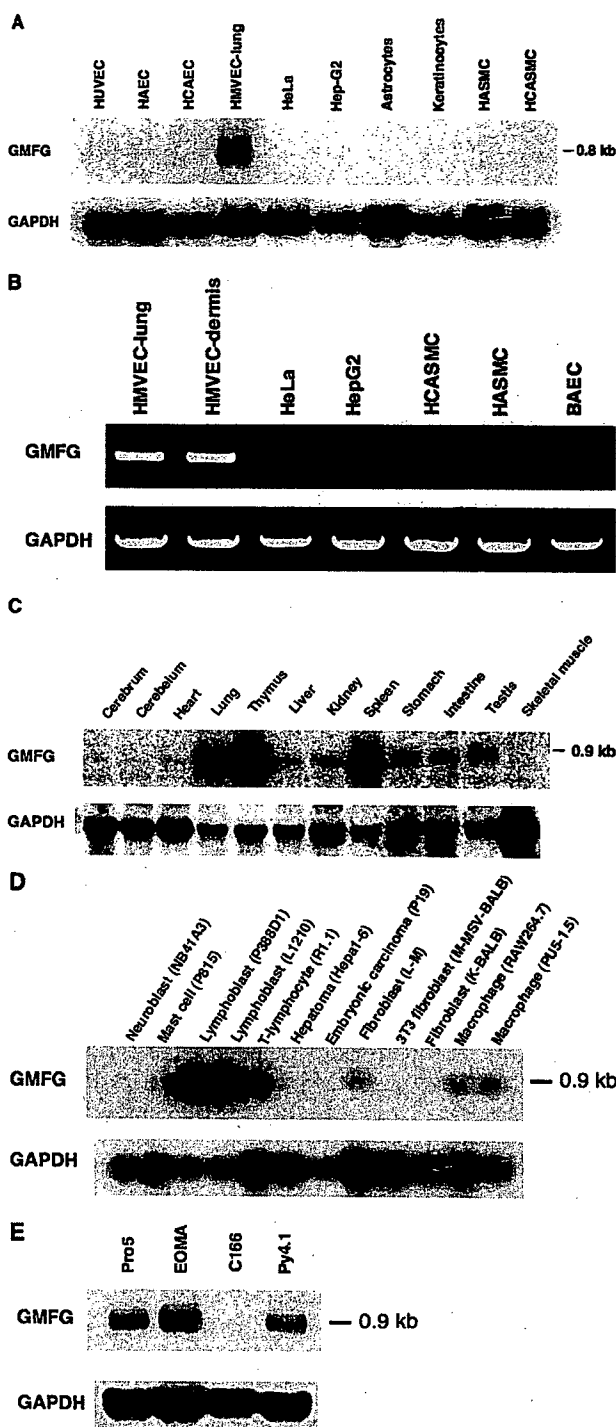


**Figure 1.** GMFG is expressed in specific types of cells. A, Northern blot analysis of GMFG in primary cultured human endothelial cells and other cultured human cells. Cells examined were human umbilical vein endothelial cells (HUVECs), human aortic endothelial cells (HAECs), human coronary artery endothelial cells (HCAECs), human lung microvascular endothelial cells (HMVEC-lung), human epithelial tumor cells (HeLa), human hepatoma cells (Hep-G2), human astrocytes, human keratinocytes, human aortic smooth muscle cells (HASMCs), and human coronary artery smooth muscle cells (HCASMCs). B, RT-PCR analysis of GMFG. HMVEC from dermis expressed GMFG as much as HMVEC-lung, whereas bovine aortic endothelial cells (BAECs) expressed minimal amount of GMFG. C, Northern blot analysis of GMFG in mouse tissues. D, Northern blot analysis of GMFG

### Mouse Ischemia/Reperfusion Model

The mice underwent pre-anesthesia with a single intraperitoneal injection of sodium pentobarbital (25 mg/kg). Following endotracheal intubation, a thoracotomy incision through the fourth intercostal space was made. The left anterior descending (LAD) coronary artery was occluded for 30 minutes then reperused for 24 hours. At the end of the experiments, the chest was opened and the left ventricles were immediately excised followed by snap freezing for RNA extraction.

### Statistics

Differences between groups were analyzed using student's *t* test;  $P < 0.05$  was considered significant. Data are presented as mean  $\pm$  SE as indicated.

### Results

#### Glia Maturation Factor- $\gamma$ Is Preferentially Expressed in Microvascular Endothelial and Inflammatory Cells

During a series of microarray studies aimed at isolating unique endothelial cell genes, we identified previously uncharacterized GMFG as being expressed only in microvascular endothelial cells derived from human lung but not by endothelial cells from other vascular beds or nonendothelial cells (Figure 1A). Amino acid sequence of GMFG is highly conserved among species, eg, 95% homology between human and mouse and 98% homology between human and bovine. GMFG was also expressed in dermal microvascular cells as much as in lung microvascular endothelial cells, and minimal expression was observed in hepatoma cells, vascular smooth muscle cells, and endothelial cells from bovine aorta, assessed by RT-PCR (Figure 1B). The primers used were of 100% match for both human and bovine GMFG. In adult mouse tissues, GMFG was expressed abundantly in thymus and spleen as well as in lung (Figure 1C). We found that GMFG was expressed in inflammatory cells such as lymphoblasts, T lymphocytes, and macrophages, a finding that is consistent with its high expression in thymus and spleen (Figure 1D). Mouse endothelial cell lines derived from normal yolk sac (Pro5), endothelioma (EOMA), and microvessels of an SV40T transgenic mouse (py4.1) also expressed GMFG (Figure 1E).

During mouse embryogenesis, GMFG was expressed as early as embryonic day 9.5 (e9.5) (Figure 2A), predominantly in blood islands of the yolk sac, in endothelial and hematopoietic cells, and possibly in the angioblast precursors to these lineages (Figure 2B through 2G). Negative control study using sense RNA probe did not show such a significant hybridization signals (Figure I in the online data supplement, available at <http://circres.ahajournals.org>). These results suggest that GMFG has a function in embryonic vasculogenesis as well as in hematopoiesis and that its expression might be well preserved during differentiation, which could account

in mouse cell line MTN blot (BD Clontech). E, Northern blot analysis of GMFG in mouse endothelial cell lines. Cells examined were Pro5 (endothelial-like cells isolated from embryonic yolk sac of a normal mouse), EOMA (mouse endothelioma cell line), py4.1 (derived from microvessels of an SV40T transgenic mouse), and C166 (isolated from embryonic yolk sac of a pro-oncogene transgenic mouse).